INSTITUTO POLITÉCNICO
DE BRAGANÇA
Escola Superior Agrária

UNIVERSIDADE TECNOLÓGICA FEDERAL DO PARANÁ

Valorization of tangerine peels in the preparation of adsorbents for removal of Ni(II) from aqueous solutions

Vitor da Costa Marques

Dissertation submitted to Escola Superior Agrária de Bragança to obtain the Degree of Master in Tecnologia Ambiental under the scope of the double diploma with Universidade Tecnológica Federal do Paraná.

Supervised by

Prof. Dr. Helder Teixeira Gomes

Dr. José Luis Díaz de Tuesta

Prof. Drª. Tatiane Cristina Dal Bosco

Bragança

2020

I dedicate this work to my parents, Edson and Claudete, to my brother Leandro and especially to my niece and goddaughter Valentina, for their unconditional support and encouragement.

ACKNOWLEDGMENTS

First of all, I would like to thank my parents, Edson and Claudete, without whom I would not be given so many opportunities, I thank you for the support and encouragement during all these years of graduation and for sharing with me the challenges and difficulties faced away from home.

I thank my brother for the partnership, complicity, for being present even with the distance.

I thank my friends Pedro and Larissa, for their support during this stage and for their friendship over the years.

To my supervisor, teacher and friend Tatiane, for all the help, advice and opportunities during the undergraduate years and later with the master's degree.

I am grateful to my co-supervisor José, who was fundamental in the execution of this work and for whom I learned to cultivate respect and admiration.

I thank my supervisor, Professor Helder, for the opportunity and confidence.

My laboratory friends Fernanda, Adriano and Gabriel, who shared their knowledge and helped me with the execution of my practical work.

I thank Maria João, technician at the Chemical Process Laboratory, for being helpful and patient.

I would like to thank Professor Margarida and the Mountain Research Center (CIMO) for their assistance with my analysis.

I am grateful to the Foundation for Science and Technology (FCT, Portugal) for financial support by national funds FCT/MCTES to CIMO (UIDB/00690/2020).

FCT Fundação para a Ciência e a Tecnologia

REPÚBLICA PORTUGUESA

NORTE2020

PORTUGAL 2020

UNIÃO EUROPEIA
Fundo Europeu de Desenvolvimento Regional

Abstract

The discharge of industrial and domestic wastewater is one of the main causes of contamination of water bodies by heavy metals. Among these heavy metals, nickel (Ni) is one of the most used in industrial processes, such as the production of alloys, stainless steel and automotive batteries, as well as electroplating activities, causing high concentrations in the effluents of these industries. Several techniques, such as chemical precipitation and filtration, have been studied in order to promote the removal of these heavy metals from wastewater. However, these techniques are often financially and technically costly. Under this context, adsorption using activated carbons (ACs) appears as an alternative, which is characterized by being an effective and economically viable technique. Citrus fruits, such as tangerine, are of great importance in the Portuguese economic context. In 2017, just over 374.4 thousand tons were produced, with 10% of this volume corresponding to tangerine. This research aimed, therefore, to produce ACs from tangerine peels and use them in the adsorption of nickel from aqueous medium. The ACs were produced in two stages: activation and carbonization. Upon activation, the hydrothermal carbonization process (HTC) was used considering $FeCl_3$ as activating agent under three concentrations (0.5, 1.0 and 2.5 M). Afterwards, the prepared materials were carbonized in a tubular oven at 800 ºC for 4 h. The samples were named as follows: TW-C (pyrolyzed peels without HTC), TW-Fe-0.5-C / TW-Fe-1.0-C / TW-Fe-2.5-C (HTC and pyrolyzed peels) and TW-Fe-2.5 (peels with HTC without pyrolysis). The physico-chemical properties of the ACs, such as elemental analysis, ash content, acidity and basicity, were determined to correlate with their performance. The kinetic and isotherm adsorption of Ni(II) onto the ACs was assessed at the following operating conditions: 2.5 g L^{-1} of AC, 25 ºC and pH 6 and modelled by the kinetic models of pseudo-first order, pseudo-second order and Elovich, as well as the adsorption isotherms of Langmuir, Freundlich and the General Isotherm Equation (GIE) of Tóth. The materials TW-C showed the best adsorption results and removed 99% of Ni(II) at pH 9. The kinetic models that best described the adsorption process were pseudo-second order (TW-Fe-2.5-C) and Elovich (TW-C). The GIE of Tóth showed the best fit, however, its parameters did not show statistical significance at the 5% confidence level, being rejected. The Freundlich model was able to represent the experimental data with certain precision (R^2 reached 0.9557 and 0.9785 for TW-C and TW-Fe-2.5-C, respectively) and statistical significance according to the t-test and F-test.

Key words: adsorption; heavy metals; nickel; valorization of solid waste; wastewater treatment.

Resumo

A descarga de águas residuais industriais e domésticas é uma das principais causas de contaminação de corpos d'água por metais pesados. Entre esses metais pesados, o níquel (Ni) é um dos mais utilizados em processos industriais, como na produção de ligas metálicas, aço inoxidável e baterias de automóveis, bem como na galvanoplastia, originando altas concentrações nos efluentes dessas indústrias. Várias técnicas, como precipitação química e filtração, foram estudadas para promover a remoção desses metais pesados de águas residuais. No entanto, essas técnicas são financeiramente e tecnicamente caras. Como alternativa surge a adsorção utilizando carvão ativado (AC), caracterizada por ser uma técnica eficaz e economicamente viável. Os citrinos, como a tangerina, apresentam relevada importância no contexto económico português. No ano de 2017 foram produzidas pouco mais de 374,4 mil toneladas, onde 10% desse volume correspondeu a tangerina. Tendo este enquadramento em consideração, este trabalho objetivou produzir ACs a partir de cascas de tangerina para aplicação na adsorção de níquel presente em meio aquoso. Os ACs foram produzidos em duas etapas: Ativação e Carbonização. Na ativação foi usado o processo de carbonização hidrotérmica (HTC) considerando $FeCl_3$ como agente ativante em três concentrações (0,5; 1,0 e 2,5 M); posteriormente, os materiais preparados foram carbonizados em forno tubular a 800 ºC por 4 h. As amostras foram nomeadas da seguinte forma: TW-C (cascas pirolisadas sem HTC), TW-Fe-0,5-C / TW-Fe-1,0-C / TW-Fe-2,5-C (HTC e cascas pirolisadas) e TW-Fe-2,5 (cascas com HTC sem pirólise). As propriedades físico-químicas dos ACs foram determinadas por análise elementar, teor de cinzas, acidez e basicidade, para correlacionação com o seu desempenho no processo de adsorção. A cinética de adsorção e isotérmicas de adsorção de Ni(II) nos ACs foi avaliada nas seguintes condições operacionais: 2,5 g L^{-1} de AC, 25 ºC e pH 6, aplicando os modelos cinéticos de pseudo-primeira ordem, pseudo-segunda ordem e Elovich, bem como as isotérmicas de adsorção de Langmuir, Freundlich e a Equação Geral da Isotérmica (GIE) de Tóth. O carvão TW-C apresentou os melhores resultados de adsorção e removeu 99% de Ni(II) a pH 9. Os modelos cinéticos que melhor descreveram o processo de adsorção foram o de pseudo-segunda ordem (TW-Fe-2.5-C) e Elovich (TW-C). O GIE de Tóth apresentou o melhor ajuste, no entanto, os seus parâmetros não apresentaram significância estatística no nível de confiança de 5%, sendo rejeitado. O modelo de Freundlich foi capaz de representar os dados experimentais com certa precisão (R^2 atingiu 0,9557 e 0,9785 para TW-C e TW-Fe-2,5-C, respectivamente) e significância estatística de acordo com o teste t e o teste F.

Palavras-chave: adsorção; metais pesados; níquel; tratamento de águas residuais; valorização de resíduos sólidos.

SUMMARY

Index of figures

Index of tables

LIST OF ABBREVIATIONS

HTC	Hydrothermal Carbonization
WHO	World Health Organization
AC	Activated Carbon
GAC	Granular Activated Carbon
FAO	Food and Agriculture Organization of the United Nations
INE	(Portuguese) National Institute of Statistics
IUPAC	International Union of Pure and Applied Chemistry
CONAMA	(Brazilian) National Council for the Environment
TOC	Total Organic Carbon
Q_e	Amount of substance adsorbed at equilibrium (mg g^{-1})
V	Volume of solution (L)
C_0	Initial concentration of the adsorbate in the solution (mg L^{-1})
C_e	Concentration of the adsorbate remaining in solution after the equilibrium (mg L^{-1})
W	Amount of adsorbent (g)
Q_t	Amount of substance adsorbed at time t (mg g^{-1})
C_t	Concentration of the adsorbate in the solution at time t (mg L^{-1})
K_L	Langmuir coefficient, related to the affinity of the solute for the adsorbent (L g^{-1})
K_f	Freundlich coefficient, an intercept that indicates the ability of the adsorbent to retain the solute.
α	Tóth isotherm constant (L^{ma} g^{-ma})
m_a	Tóth isotherm constant

$\boldsymbol{m_k}$	Tóth isotherm constant
$\boldsymbol{k}$	Tóth isotherm constant (L^{mk} g^{-mk})
$\boldsymbol{\alpha}$	Initial sorption rate of the Elovich kinetic model (mg g^{-1} min^{-1})
$\boldsymbol{\beta}$	Constant related to the extent of surface coverage and activation energy for chemisorption (g mg^{-1})
$\boldsymbol{\alpha_{prob}}$	Level of statistical significance

1 INTRODUCTION

Water is the most common substance in nature and a wide range of natural and human influences can affect its quality. Contamination of water bodies by heavy metals has become a serious health and environmental problem owing to the toxicity and non-biodegradability of these pollutants[1,2]. Heavy metals can enter into the aquatic system through natural phenomena and anthropogenic actions, with the main sources being the release of domestic and industrial wastewater, atmospheric phenomena and the weathering of rocks and soils[3,4].

Among heavy metals, nickel (Ni) is one of the most used in industrial processes, such as smelting, stainless steel and battery manufacturing[5,6,7]. Thus, it is among the most common pollutants found in industrial wastewater[8]. In drinking water, nickel can cause health problems when it is found in quantities above the limit set by the World Health Organization (WHO), which is 0.07 mg L^{-1}. Dermatitis is the main problem caused by exposure to nickel. Moreover, acute poisoning by this metal can cause headaches, dizziness, vomiting, cyanosis and extreme weakness[8,9,10].

In view of the above, it is necessary to adopt measures that aim the removal of these contaminants present in wastewater. Many techniques have been used to remove heavy metals from water, such as membrane filtration[11], chemical precipitation[12], ion exchange[13] and electrochemical treatment[14]. However, these techniques are usually expensive and non-ecofriendly[7]. On the other hand, adsorption has the benefits of being a low-cost and effective technique for a variety of metals, existing at present a wide range of potential biodegradable adsorbent materials[15].

Activated carbons (ACs) show high performances as adsorbents in the adsorption process. ACs are carbon-rich materials produced from the pyrolysis of organic matter in an oxygen-free environment[16] and it can be obtained from various organic residues, such as agricultural wastes, which are renewable and generally available in large quantities[17,18,19]. Citrus peels are a potential biomass waste for the production of ACs, considering the volume of citrus fruits produced and the problems related to the disposal of these residues. In Portugal, in 2017, 374.4 thousand tonnes of citrus fruits were produced, including 37 thousand tonnes of tangerine and 15 thousand tonnes of lemon, placing the citrus fruits as the second group of products most exported[20].

Given the above considerations, the aim of this research is to perform the production of ACs from the peel of tangerine and to evaluate its efficiency in the removal of nickel from aqueous solutions.

1.2 Objectives

1.2.1 General

To evaluate the production of activated carbons from tangerine peels and to assess their performance in the adsorption of Nickel, used as model heavy metal pollutant.

1.2.2 Specific aims

- To prepare carbon-based materials from tangerine peels.
- To characterize the physico-chemical properties of each prepared material.
- To assess the efficiency of nickel removal from aqueous solution by determination of adsorption isotherms with the best produced ACs.
- To study the nickel adsorption kinetics and the equilibrium adsorption isotherms with the best ACs.

1.3 Document structure

This master thesis is divided into five chapters. Chapter 1 presents the introduction and objectives of the work, when relevant topics are raised for the understanding of the theme regarding the contamination of water bodies by heavy metals and their treatment by adsorptive processes using activated carbon prepared from agro-industrial waste.

Chapter 2 presents the state of the art, part of the work where the bibliographic survey was carried out with regard to the recovery of waste, the citrus industry, the preparation of activated carbon, the contamination of water bodies with nickel resulting from the wastewater discharge, in addition to revising kinetics and adsorption isotherms.

The experimental part of the work is detailed in chapter 3, where the reagents, equipment and experimental processes are described.

The results obtained for the characterization of activated carbon and raw material, kinetics and adsorption isotherms are presented in chapter 4.

Finally, chapter 5 presents the conclusions with topics of interest for future research.

2 STATE OF THE ART

2.1 Solid waste valorization

According to the directive 2008/98/CE (amended by directive 2018/851), waste is "any substances or objects that the holder disposes of or has the intention or obligation to dispose of" and, therefore, the adoption of techniques that aim at the reuse or even the valorization of this waste become extremely important in view of the need to reduce the amount of natural resources and energy used. The management of solid waste is one of the biggest challenges currently faced, as its management and final disposal can cause serious environmental impacts, such as soil and water contamination by solid waste landfill[21].

The directive mentioned above still establishes the waste hierarchy, which aims to reduce the amount of waste going to landfills (Figure 1) that applies as follows: a) Prevention and reduction; b) Reuse; c) Recycling; d) Other types of recovery, for example energy recovery; and e) Elimination.

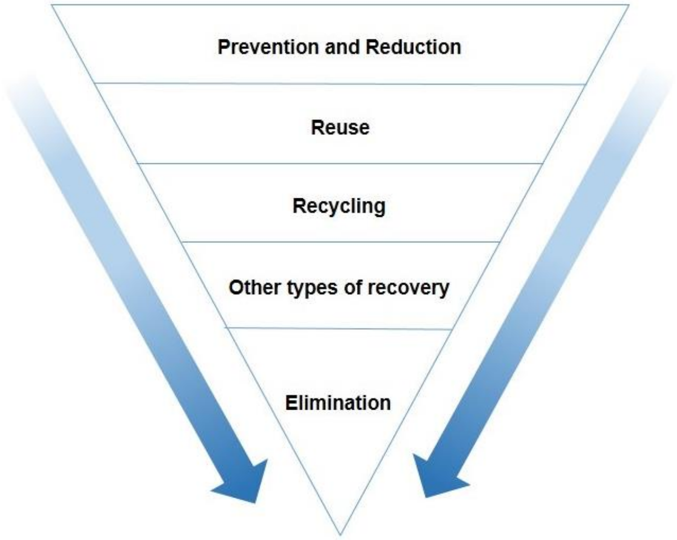

Figure 1. Waste hierarchy according to directive 2008/98/CE.

The stages of elimination, recycling, recovery (or valorization) and treatment are applied at different times in the solid waste management process and there is common confusion among the definitions of these terms. According to the directive, elimination is "any operation that is not recovery, even if it has the secondary consequence of recovering substances or energy", recycling is defined as "any recovery operation through which the materials that make up waste are again transformed into products, materials or substances for their original purpose or for other purposes", the recovery step is" any operation whose main result is the transformation of waste in order to serve a useful purpose, replacing other materials" and finally treatment, which is "any recovery or disposal operation, including preparation prior to recovery or disposal".

Following the global trend, Brazil enacted Law No. 12,305, in 2010, that instituted the national solid waste policy and "provides for its principles, objectives and instruments, as well as guidelines for integrated management and solid waste management, including the dangerous ones, the responsibilities of generators and public authorities and the applicable economic instruments". In its article 15, goals were established such as reduction, reuse, recycling, among others, in order to reduce the amount of waste generated, as well as the amount of waste sent to landfills[22].

Table 1 shows the main forms of waste treatment applied in the European Union. As expected, the total amount of waste generated is related to the population and economic size of a country.

Table 1. Solid waste treatment in the European Union in 2016.

	Valorization[1]			**Disposal[1]**		**Total waste generation (million tonnes)**
	Recycling %	**Backfilling[2] %**	**Energy recovery %**	**Landfill and other %**	**Incineration without energy recovery %**	
EU-28	37.8	9.9	5.6	45.7	1	842.94
Belgium	76.9	0	12.6	6.4	4.1	35.66
Bulgaria	5.2	0	0.4	94.4	0	17.65
Czech	49.5	29	4.5	16.6	0.4	11.98
Denmark	51.4	0	19.5	29.1	0	8.96
Germany	42.7	26.6	11.3	18.1	1.2	142.49
Estonia	21.6	11.2	2.5	64.7	0	2.13
Ireland	10.6	46	4.8	38.4	0.3	7.94
Greece	4.8	0	0.3	94.8	0	13.80
Spain	37.1	5.7	3.6	53.6	0	65.88
France	55	10.3	5.4	27.6	1.6	90.14
Croatia	47.2	4	1	47.8	0	3.30
Italy	78.9	0.1	4	14.2	2.7	100.27
Cyprus	10.4	28	3.8	57.8	0	0.68
Latvia	71.7	1.1	6.8	20.3	0	2.01
Lithuania	33.4	4.1	5.8	56.6	0	3.35
Luxembourg	34.8	24.2	2.1	39	0	1.37
Hungary	54.1	3.7	7.4	34.2	0.6	10.55
Malta	19.1	63.4	0	17.2	0.4	0.43
Netherlands	45.6	0	7.6	46	0.9	41.09
Austria	37	11	:	45.9	:	15.54
Poland	46.2	22.2	3.3	28	0.4	77.95
Portugal	43.5	9.5	12.1	34.7	0.2	11.04
Romania	4	0.4	1.4	94.1	0.1	20.89
Slovenia	60.2	27.2	4.8	6.9	0.8	2.90
Slovakia	40	4.7	7	47.8	0.5	7.58
Finland	7.4	0	4.5	88	0	13.46
Sweden	12	4.9	6.6	76.3	0.2	19.55
United Kingdom	48.5	7.8	3.4	37.5	2.7	114.17

Note[1]: In mass.

Note[2]: the use of waste in excavated areas for the purpose of slope reclamation or safety or for engineering purposes in landscaping.

Source: Eurostat 2016.

Portugal has shown a gradual improvement over the years with regard to the correct disposal of waste. In 2002, the uncontrolled disposal in dumps was eradicated, being replaced by landfills. However, in 2012, just over 54% of all urban waste generated in mainland Portugal was sent to these landfills, a characteristic observed in most European countries, despite the waste hierarchy recommending that this should be the last option in the destination of solid waste[23].

The fourth and penultimate stage in the hierarchy of solid waste management is recovery, that is, the transformation of a waste so that it has a useful purpose. The production of activated carbon can be seen as a way of valuing waste, as it allows the replacement of commercial activated carbon that is more expensive when compared to activated carbon produced from waste[24].

2.2 Production of citrus fruits

Citrus fruits are one of the largest fruit crops in the world. Similarly, the citrus industry is also the second largest fruit processing industry, surpassed only by the grape industry, which mainly produces wine[25]. The genus *"Citrus"*, according to the system of plant taxonomy, belongs to the family *Rutaceae* and they are plants originating in the tropical and subtropical southeast of Asia[25,26].

As reported by FAO (Food and Agriculture Organization of the United Nations)[27], in the year of 2016, 124,246.0 thousand tonnes of citrus fruits were produced in the world. Among that, 32,968.5 thousand tonnes were tangerine and 15,981.8 thousand tonnes were lime and lemon. Table 2 shows the countries with the largest citrus fruits production in the world.

Table 2. The five largest citrus fruits producers in the world.

Country[1]	2012	2013	2014	2015	2016	Participation (%)
China	31,830.4	34,261.7	36,467.0	38,153.9	32,705.9	26.3
Brazil	20,258.5	19,734.7	19,073.9	18,921.6	16,555.1	13.3
India	6,955.0	9,235.0	10,401.1	9,216.2	9,755.8	7.9
USA	10,813.0	10,301.0	8,751.0	8,208.0	7,829.0	6.3
Spain	5,553.8	6,685.7	7,041.6	6,100.5	6,882.0	5.5
World	123,002.3	128,611.1	131,707.7	130,947.0	124,246.0	100.0

Note[1]: Total production of citrus fruits in thousand tonnes.
Source: FAO (2017)[27].

According to the portuguese National Institute of Statistics (INE) and the Ministry of Agriculture, Forestry and Rural Development[28], in Portugal, the production of citrus fruits (orange, lemon, tangerine and grapefruit) is very important in the national economic context. In 2016, the group of exported products in which citrus fruits are included presented the 2nd place as being the most commercialized, with the main buyers being Spain, France, and Germany.

In Figure 2 is shown the data about the area used for citrus fruits cultivation in Portugal and the total production in the period between 2000 and 2017.

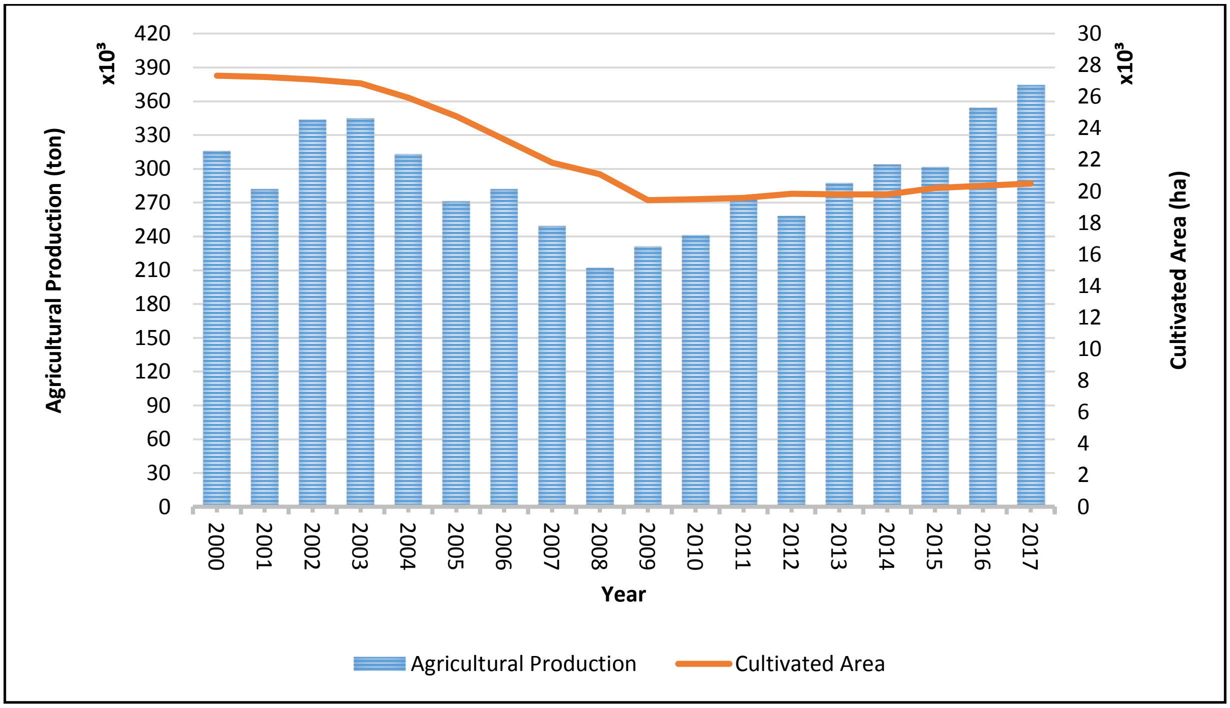

Figure 2. Cultivated areas with citrus fruits and citrus fruits production in Portugal in the years 2000-2017. **Source:** INE/PORDATA (2018)[20].

In the year 2017, a little more than 374.4 thousand tonnes of citrus fruits were produced in Portugal, of which 37 thousand were tangerine and 15 thousand were lemon. In the same year, the Algarve region was responsible for producing 309,028 tonnes, equivalent to 82.5% of the total production, making the region the largest producer of citrus fruits in Portugal[29].

In addition to the economic importance of citrus fruits, due to the good acceptance by consumers, they play an important role in human nutrition, considering the wide range of phytochemicals present in their composition, such as flavonoids, which are compounds that play antiallergic, anti-inflammatory and antimicrobial roles[30].

Most citrus fruits are used by processing industries for juice production and after processing these fruits, large amount of waste is generated, being the main waste seeds and peels[31]. It is noteworthy that due to the amount of organic matter present in citrus fruits peels, the disposal of this type of residue directly in the soil can cause damage, given its ability to change the physicochemical characteristics of the soil[32].

2.3 Biochar and activated carbon

Biochar is a carbon-rich byproduct produced from the pyrolysis of organic matter in an environment free of oxygen[16]. Agricultural waste is a raw material widely studied for this purpose since it is renewable and available in large quantities[17,18]. On the other hand, activated carbon is obtained from the activation of the material resulting from the pyrolysis, in the presence of oxidizing agents[33]. Activated carbon can be obtained from a variety of raw materials, as long as they have high carbonaceous content.

In the process of biochar production two steps are performed: pyrolysis, which can be classified as “slow” and “fast”, and the activation step itself. The differentiation between fast and slow pyrolysis is the time of permanence of the vapor: in the slow pyrolysis the residence time is longer and the temperatures are lower[34].

According to Bridgwater (2012)[34], three by-products are generated in the process of pyrolysis, *viz.* gases, bio-oil and the biochar. The process of pyrolysis performed at lower temperatures and longer residence times (slow pyrolysis) favors the formation of biochar. High temperatures and longer residence times (fast pyrolysis) favors the formation of gases, while moderate temperatures and short residence times favor the formation of bio-oil.

The different products obtained by the different pyrolysis modes are shown in Figure 3 and in Table 3. It is possible to observe how the change of the process conditions can lead to the formation of different products.

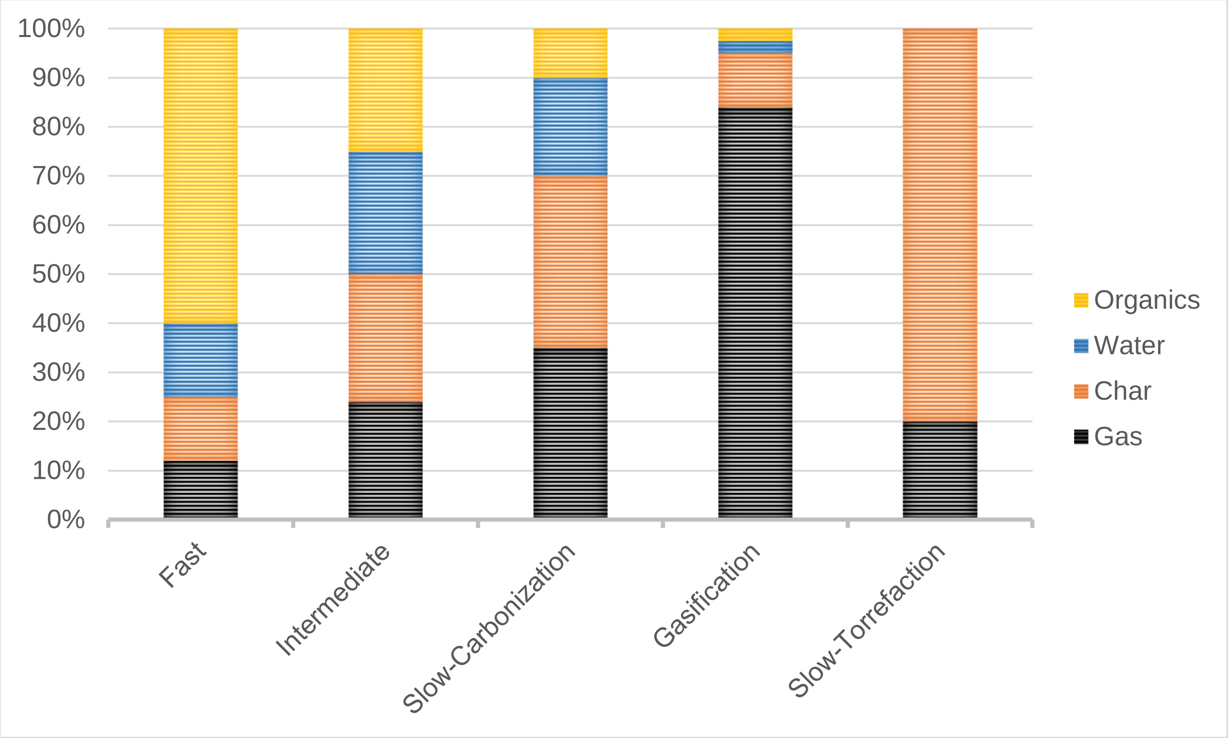

Figure 3. Pyrolysis methods and yields of the respective products.
Source: Adapted from BRIDGWATER (2012)[34].

Table 3. The yield of the products (dry wood base) obtained by the different pyrolysis modes.

Mode	Conditions	Liquid	Solid	Gas
Fast	≈ 500 ºC, short hot vapor residence time ≈ 1 s	75%	12% char	13%
Intermediate	≈ 500 ºC, hot vapor residence time ≈ 10-30 s	50% in 2 phases	25% char	25%
Carbonization (slow)	≈ 400 ºC, long vapor residence hours → days	30%	35% char	35%
Gasification	≈ 750-900 ºC	5%	10% char	85%
Torrefaction (slow)	≈ 290 ºC, solids residence time ≈ 10-60 min	0% unless condensed, then up to 5%	80% char	20%

Source: BRIDGWATER (2011)[34].

There are two types of activation strategies to prepare activated carbons: physical and chemical activation. According to Angin et al. (2013)[35], in the physical activation the raw material is first carbonized and the carbonized material is then activated by vapor or carbon dioxide. In the chemical activation the raw material is impregnated with an activating agent and the impregnated material is thermally treated under an inert atmosphere.

Activated carbons prepared by the activation of raw biomass is an attempt to develop a cost-effective and efficient adsorbent alternative to costly coal-based commercial activated carbons[36]. It is widely used in environmental applications for the removal of impurities from gases and liquids due to its high adsorption capacity. The internal pore properties, such as specific surface area, pore volume and pore size distribution are the responsible for the high adsorptive capacities of activated carbons[37,38].

According to the International Union of Pure and Applied Chemistry (IUPAC), activated carbons are classified as:

- Microporous: containing pores up to 20 Å.
- Mesoporous: containing pores between 20 to 500 Å.
- Macroporous: containing pores over 500 Å.

All activated carbons present micro, meso and macropores, but their quantity and distribution can be very variable.

Activated carbons have several important utilities, such as purification of contaminated streams, removal of flavors and odors from water for domestic and industrial supply and wastewater treatment[35].

Recently, many studies have been carried out to evaluate the efficiency of activated carbons in the adsorption of pollutants in water for domestic supply and industrial wastewater. In a study performed by Özsin et al. (2019)[39], an activated carbon was produced from chickpea (*Cicer arietnum)* husks by chemical activation with KOH and K_2CO_3 and its feasibility evaluated in the removal of heavy metals from aqueous solutions. As a result, the authors concluded that the activated carbon prepared by KOH reveals a relatively high specific surface area (2.082 $m^2\ g^{-1}$ with KOH activation, against 1.778 $m^2\ g^{-1}$ with K_2CO_3 activation), as well as high adsorption of Pb(II), Cu(II) and Cr(IV), depending on the conditions used, namely pH, adsorbent dose, initial metal concentration, and concentration time.

2.2.1 Hydrothermal Carbonization (HTC)

Basically, hydrothermal carbonization is a thermochemical conversion technique that uses water and autogenous pressure for the conversion of wet/dry biomass to carbonaceous products. Normally, a temperature range of 150 to 350 ºC is used[40,41,42,43].

The main product obtained from HTC is a solid called hydrochar. This material can be used as biofuel or for other purposes, as for example for soil amendment, as a biocatalyst or for water treatment[44]. Hydrochars, are different from biochars, both chars having different chemical structure and composition[45].

One of the main advantages of hydrothermal carbonization is the use of aqueous solutions under high temperature and autogenously generated pressure[46]. Under these conditions water acts as a solvent, reagent or even as a catalyst and therefore no pre-drying of a raw material is required[47].

The HTC process is interesting due to its simplicity, low-cost and its energy efficiency[48]. As discussed in the previous section, ACs are produced from chemical or physical activation processes using biomass as precursors. The possibility to reduce production costs by improving the energy efficiency of the process would be very interesting[43]. Therefore, the combination of hydrothermal carbonization and activation processes becomes interesting when cost reduction is aimed.

Hydrochars contain rich functional groups that can greatly improve hydrophilicity and chemical reactivity[49]. Because of this, many scientists have been testing HTC-derived carbonaceous materials as adsorbents for the removal of heavy metals, pesticides, and drug residues[50].

Erdogan et al. (2015)[51] evaluated the properties of hydrochars produced from orange pomace under different temperatures and residence times and observed that with the increase of temperature, the C/H ratio tends to decrease, suggesting the predominance of dehydration reactions during the process. Several reactions may occur during the HTC process, including primary reactions of hydrolysis, dehydration, decarboxylation, aromatization and polymerization[52].

2.4 Preparation of activated carbons from citrus fruit wastes

Approximately one third of the citrus fruits are processed, resulting in 50–60% of organic waste which is typically constituted by the peel, seeds and leaf residues remaining after the juice extraction process[31]. In the processing of citrus fruits, different types of solid waste and liquid effluents are generated. Solid waste consists of peels, rags, seeds and sludge. Liquid effluents contain factory effluents, fruit wash wastewater and floor wash water[53].

There are numerous uses for the waste and by-products of the processing of citrus, among them, animal feed, oil extraction, biofuel production, encapsulating agent, development of biodegradable packages and finally the development of activated carbons. Since fossil fuels are nonrenewable, organic wastes can be used in the production of activated carbons, meeting the growing demand for this kind of materials[54].

Several authors have evaluated the use of citrus fruits residues as carbon precursors for the preparation of biochars and activated carbons. In Table 4 are summarized the studies that evaluated the use of these carbon-based materials prepared from citrus fruit residues as adsorbents for the removal of heavy metals and other compounds.

Table 4. Summary of the methods applied for the production of activated carbon from citric wastes.

Precursor of carbon	Method of activation	Conditions	Method of carbonization	Conditions	Ref
Orange peels	No use	-	Pyrolysis	400-800 ºC, 2 h/6 h	55
Indian sweet lime peels and seeds	Chemical activation (H_2SO_4)	Treated with concentrated sulphuric acid at 1:2 ratio by weight and kept at 160 ± 5 ºC in an air-oven for 24 h	No use	-	56
Lemon peels	Chemical activation (H_3PO_4)	It was soaked for 24 h in a solution of phosphoric acid at a ratio of 2:1 (v/v), then it was dried in an oven at 250 ºC	Pyrolysis	500 ºC during 1 h, under nitrogen flow	57
Orange peels	Chemical activation (H_2SO_4)	It was soaked for 24 h in a solution of sulphuric acid (40%)	Pyrolysis	200 ºC during 2 h in inert atmosphere of CO_2	58
Lemon peels	No use	-	Pyrolysis	500 ºC during 1 h in the presence of air	59
Orange peels	Chemical activation (KOH)	Peels were impregnated with aqueous solution of KOH (2.0 mL/g orange peel)	Pyrolysis	550 ºC during 4 h, under an argon flow	60
Grapefruit peels	Chemical activation (CH_3CH_2OH, NaOH and $MgCl_2$)	It was soaked with anhydrous ethanol, NaOH (0.5 M) and $MgCl_2$ (1.5 M)	Pyrolysis	450 ºC during 3 h, under N_2 flow	61
Orange peels	Physical activation (CO_2 or air)	It was performed under a steady flow of CO_2 (40 mL/min) at 750 ºC, or air (70 mL/min) at 300 ºC during 1.5 h	Hydrothermal Carbonization	200 ºC during 20 h	62
Orange peels	Chemical activation ($ZnCl_2$)	Activated using 1.0 M $ZnCl_2$ at 500 ºC for 3 h	Pyrolysis	400 ºC during 15 min	63

2.4.1 Adsorbents prepared from citrus fruits peels

One of the characteristics of citrus fruits is the relatively high mass proportion of peels. New technologies have been developed in order to convert this huge waste disposal problem into an additional source of income[64]. Taking into account the large amount of waste generated in the citrus juice processing industry, these organic waste represents a renewable, abundant and cheap source of biomass[54].

Given the large amount of organic matter present in citrus fruit peels, the disposal of this kind of residue directly in the soil is difficult, given the potential damage to the natural and beneficial microorganisms presented in it[32]. Table 5 shows the main constituents of different citrus fruits varieties on the dry matter weight.

Table 5. Main constituents of different citrus fruits varieties.

Citrus variety	Peel[1] (%)	Segment membranes and juice sacs[1] (%)	Seeds[1] (%)
Orange	65.4	31.8	2.2
Tangerine	75.5	22.6	0.0
Mandarin	58.2	32.6	9.2
Grapefruit	65.1	33.3	1.6
Lemon	69.6	25.0	5.3

Note[1]: Dry matter weight

Source: PASCUAL & CARMONA (1980)[65]; ZEMA et al. (2018)[66].

Guiza (2017)[67] evaluated the adsorption of Cu^{2+} from aqueous solution using orange peel and verified the presence of chemical functional groups such as carbonyls, hydroxyls, amines and amides. These groups were identified as potential adsorption sites responsible for binding the metal ions to the adsorbent. Torab-Mostaedi et al. (2013)[68] studied the biosorption of cadmium and nickel in grapefruit peels and observed that functional groups such as carboxyls and carbonyls are the main responsible for the biosorption of heavy metals. Some researchers associate the presence of functional groups such as carboxyl and phenols with the existence of cellulose, hemicellulose and lignin in this kind of residue[59,69].

The different properties presented by the fruit peels make this waste suitable as adsorbent. Heavy metals, dyes and organic pollutants can be successfully removed from an aqueous solution using fruit peels[70].

Chen and Chen (2009)[18] evaluated the adsorption of naphthalene and 1-naphthol by activated carbons prepared from the orange peel. They observed that with the increase of the temperatures employed in the pyrolysis process there was an increase in the adsorption of the mentioned compounds. The authors justified that this fact could be explained by the increase of the surface area of the carbonaceous material.

Mohammadi et al. (2014)[57] studied the removal of Malachite green dye and lead from wastewater using lemon peels and obtained removals of over 90% of the heavy metal and reported that the low cost, the fast adsorption ability and the easiness of regeneration of this adsorbent offers a promising technique for the cleaning of wastewater.

2.5 Nickel pollution

According to Koller & Saleh (2018)[71], heavy metals are natural elements presenting high atomic mass and high density, usually at least 5 g cm^{-3}. Some heavy metals, such as iron, cobalt, nickel, copper, zinc and arsenic, are essential in animals, with indispensable functions for the entire human metabolism[72]. Several studies indicate that some heavy metals are, or are at least, likely to be carcinogenic (hexavalent chromium, arsenic, cobalt, nickel, antimony, vanadium and mercury), mutagenic (arsenic and vanadium), teratogenic (arsenic), allergenic (nickel) or endocrine-disrupting (silver, copper, zinc and selenium)[71]. Low levels of nickel induce reduced growth in intrauterine development and its deficiency can reduce iron absorption and leads to anemia[73]. The main adverse effects caused by exposure to this metal and its compounds are skin allergies, lung fibrosis and lung cancer[74,4]. Not all nickel compounds are equally carcinogenic, their carcinogenic potency depends on their ability to enter cells[75].

Nickel(II) comprises about 3% of the composition of the Earth, it is one of the most abundant elements in the Earth's crust, it is the 5th most abundant by weight[76,75] and it is one of the most used in the manufacturing process of stainless steel, metallic alloys and batteries[5]. Nickel is released from various industries, like nickel plating, silver refinery, zinc-based casting industry and storage batteries, mining and metallurgy of nickel[2]. These industries can generate great amounts of effluents with the presence of organic and inorganic compounds, like nickel. When the concentration limits are reached these compounds exhibit toxic and non-biodegradable properties[2,77].

The presence of nickel in drinking water can also occur due to the corrosion of pipes containing nickel in their composition or even owing to the poorly removal of this metal by water treatment systems[78]. Regulatory environmental agencies establish concentration limits for this metal, due to the risks presented by the presence of nickel in drinking water and wastewater. In Brazil, the National Council for the Environment (CONAMA)[79], in its resolution nº 357/2005, determines as a standard of water quality the nickel concentration limit of 0.025 mg L^{-1} for freshwater classes 1, 2 and 3 and the emission limit in water bodies as being 2 mg L^{-1}. In Portugal, the Ministry of the Environment[80], in its Decree-law nº 236/1998, does not establish a maximum admissible value for freshwater destined to urban water supply. However, after treatment, the established nickel concentration limit is 0.05 mg L^{-1}. For the discharge of effluents into water bodies, the emission limit value is 2 mg L^{-1}. The WHO[81] establishes as guideline a value of 0.07 mg L^{-1} for the concentration of nickel in drinking waters.

2.6 Adsorption with activated carbons

According to Ruthven (1984)[82], adsorption is the transfer of substances (adsorbates) from a fluid phase to the surface of a solid phase (adsorbent). In this process, the molecules present in the fluid phase are adsorbed on the surface of the adsorbent due to the existence of attractive forces that are not compensated. According to IUPAC, adsorption is a surface phenomenon in which particles and/or molecules bind to the top layer of a material.

Adsorption can be divided into two classes: physical adsorption (physisorption) and chemical adsorption (chemisorption). Physical adsorption occurs through intermolecular interactions, such as Van Der Waals, between the adsorbent and the adsorbate (solute that is expected to be adsorbed). Chemisorption involves the chemical interaction between the two components[83].

There are several techniques which are used to remove contaminants from the environment, including ion exchange, precipitation, adsorption and membrane processes. Adsorption is the most promising technique since it presents a low cost and easy operation[84]. It is a technique generally used in the removal of contaminants, such as agricultural pesticides, heavy metals and substances dissolved in aqueous solutions in which the removal is rendered impracticable by conventional techniques.

Adsorption can be influenced by the properties of the adsorbent, pH, concentration of the adsorbate and the adsorbent load. These characteristics will directly affect process efficiency[85,19]. In the case of pH, the improved metal cation adsorption at higher solution pH occurs due to the lower number of H^+ ions, while at low pH, competition occurs between hydronium and metal cations, reducing the ion adsorption[36,86,87].

As illustrated in Figure 4 for adsorption of nickel, the functional groups present at the surface of activated carbons play an important role in the adsorption process. Carboxylic, phenolic and other organic functional groups are responsible for the surface reactivity of activated carbons[5].

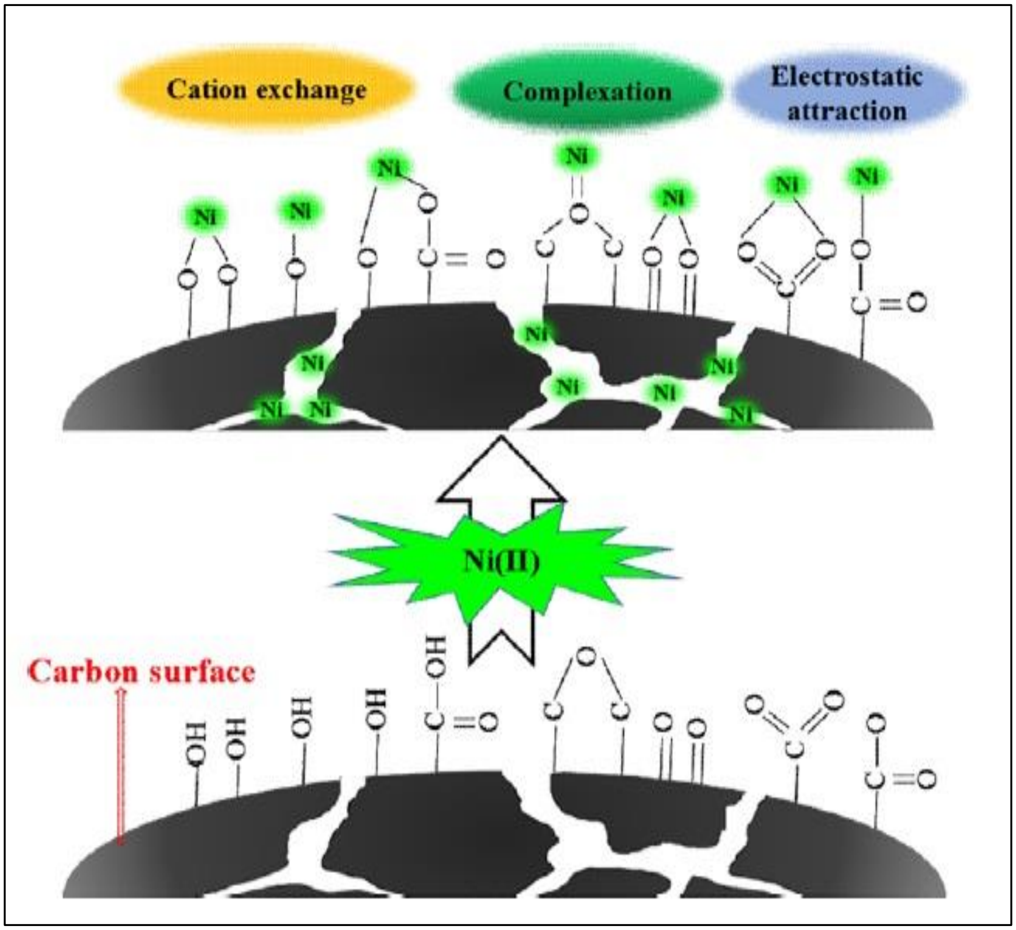

Figure 4. Graphical representation of possible adsorption mechanisms of nickel.
Source: YU et al. (2019)[6].

Kinhikar (2012) evaluated the performance of granular activated carbons unmodified and modified with nitric acid in the process of nickel adsorption and observed that the adsorption by granular activated carbon was increased after the oxidation with nitric acid. The author explains that this fact is due to the formation of additional surface functional groups that favor nickel adsorption[76].

Samarghandi et al. (2010)[88] used activated carbons obtained from holly sawdust and observed a decrease of the nickel removal in terms of percentage (48.37 to 40.45%) with the increase of nickel concentration from 40 to 80 mg L^{-1}, which can be explained by the limited amount of active sites that become saturated above certain concentrations.

Erdoğan et al. (2005)[89] studied apricot waste to produce activated carbons employing different pyrolysis temperatures (400, 500, 600, 700, 800 and 900 ºC) and observed that the activated carbon obtained at 900 ºC revealed a higher rate of nickel adsorption as well as higher surface area and pore volume.

2.7 Adsorption kinetics

Several factors can affect the adsorption process in a liquid medium, such as molecular structure or nature of the adsorbent, solubility of the adsorbate and pH solution[85,36]. The molecular structure of the adsorbent is important in ordering the degree of adsorption that affects the type and location of the functional groups responsible for the process[90].

The adsorbed amount of the adsorbate on the adsorbent at the equilibrium is calculated by the difference between the initial concentration of the adsorbate and the remaining concentration in the solution after equilibrium[91], according to Equation 1:

$$Q_e = \frac{V\,(C_0 - C_e)}{W} \tag{1}$$

where Q_e (mg g^{-1}) is the amount of adsorbate on the adsorbent, V (L) is the volume of solution, C_0 (mg L^{-1}) is the initial concentration of the adsorbate in the solution, C_e (mg L^{-1}) is the concentration of the adsorbate remaining in the solution after equilibrium and W (g) is the amount of adsorbent. In batch experiments, the amount of adsorbate on the adsorbent upon a given adsorption time is defined in Equation 2:

$$Q_t = \frac{V\,(C_0 - C_t)}{W} \tag{2}$$

where Q_t (mg g^{-1}) is the amount of adsorbate on the adsorbent at time t, V (L) is the volume of solution, C_0 (mg L^{-1}) is the initial concentration of the adsorbate in the solution, C_t (mg L^{-1}) is the concentration of the adsorbate in the solution at time t and W (g) is the amount of adsorbent.

The adsorption kinetic mechanism occurs in three main steps: (i) diffusion of the adsorbate to the outer surface of the adsorbent. In other words, the adsorbate molecules are transported from the liquid phase to the boundary layer surrounding the adsorbent; (ii) intraparticle diffusion, step in which the diffusion of the surface occurs to the active sites inside the particles, and (iii) chemical interaction or adsorption itself on the active sites via different mechanisms such as chelation, ion exchange or complexation[82].

Kinetic models are used to evaluate the behavior of the adsorbent. It is possible to know the variables that influence adsorption and predict the rate at which the pollutant is removed, being very important for the development of adequate treatment systems. The Lagergren equation, also known as the kinetic equation of pseudo-first order, was one of the first-rate equations developed for adsorption at solid surfaces in solid/liquid systems. It is widely used in adsorption processes in aqueous solution and it is based in the adsorption capacity of the solid[92].

According to Miao et al. (2016)[93], this model assumes that the rate of change of solute adsorption over time, the difference in saturation concentration and the amount of solute adsorbed as a function of time are directly proportional to time. The Lagergren equation is presented in Equation 3,

$$Q_t = Q_e(1 - e^{-k_1 t}) \tag{3}$$

where Q_e (mg g^{-1}) and Q_t (mg g^{-1}) are the amounts of substance adsorbed at equilibrium and at time t (min), respectively, and k_1 (min^{-1}) is the constant of the adsorption rate.

The kinetic model of pseudo-second order is also based in the adsorption capacity of the solid phase and demonstrates the behavior of the process over the entire contact time band[92].

The advantage of this model is that it is not necessary to know the equilibrium capacity in the experiment, since it can be calculated[94]. The pseudo-second order model is described in Equation 4,

$$Q_t = \frac{Q_e^2\, k_2\, t}{1 + Q_e\, k_2\, t} \tag{4}$$

where Q_e (mg g^{-1}) and Q_t (mg g^{-1}) are the amounts of substance adsorbed at equilibrium and at time t (min), respectively, and k_2 (g mg^{-1} min^{-1}) is the adsorption rate constant of pseudo-second order.

Several authors have used the kinetic models of pseudo-first and pseudo-second orders to investigate the mechanism of adsorption of heavy metals with different adsorbents[6,39,88,95,96,97,98].

Another model widely used to describe the kinetics of adsorptive processes is the Elovich model. The Elovich equation Equation (5) considers an exponential decrease in the adsorption rate with the increase in the adsorbed amount and is usually used to determine the chemisorption kinetics in heterogeneous solid supports[99].

$$Q_t = \left(\frac{1}{\beta}\right) ln(1 + \alpha\, \beta\, t) \tag{5}$$

where Q_t (mg g^{-1}) is the amount of substance adsorbed at time t (min), β (g mg^{-1}) is the constant related to the extent of surface coverage and activation energy for chemisorption, α (mg g^{-1} min^{-1}) is the initial sorption rate.

According to Liu et al. (2008)[100] the intercept (absolute value of α) of the Elovich equation indicates the ability of the adsorbent, that is, the larger is the value of α, the stronger is the ability for adsorption. Many authors have also used the Elovich model to study the adsorption kinetics of heavy metals[100,101,102,103].

2.8 Equilibrium adsorption isotherms

Starting from solutions with different solute concentrations, the concentrations of the solute adsorbed on the solid phase (Q_e) and the concentrations of solute remaining in the solution after the equilibrium (C_e) represent pairs of coordinates distributed in the Cartesian plane, an adsorption isotherm being thus obtained.

Giles et al. (1974)[104] classified sorption isotherms for solutes, relating their characteristic shapes to parameters of the solvent. They are distinguished between four isotherm classes: high affinity (H), Langmuir (L), constant partition (C) and sigmoidal-shaped (S), as shown in Figure 5.

According to Hinz (2001), “S isotherms have a concave shape at low concentrations. While both H and L isotherms have a convex shape, the slopes of H isotherms reach high values whereas slopes of L isotherms remain constant. This indicates that the sorption affinity of H isotherms increases with decreasing concentration. C isotherms are defined by a constant sorption affinity".[105]

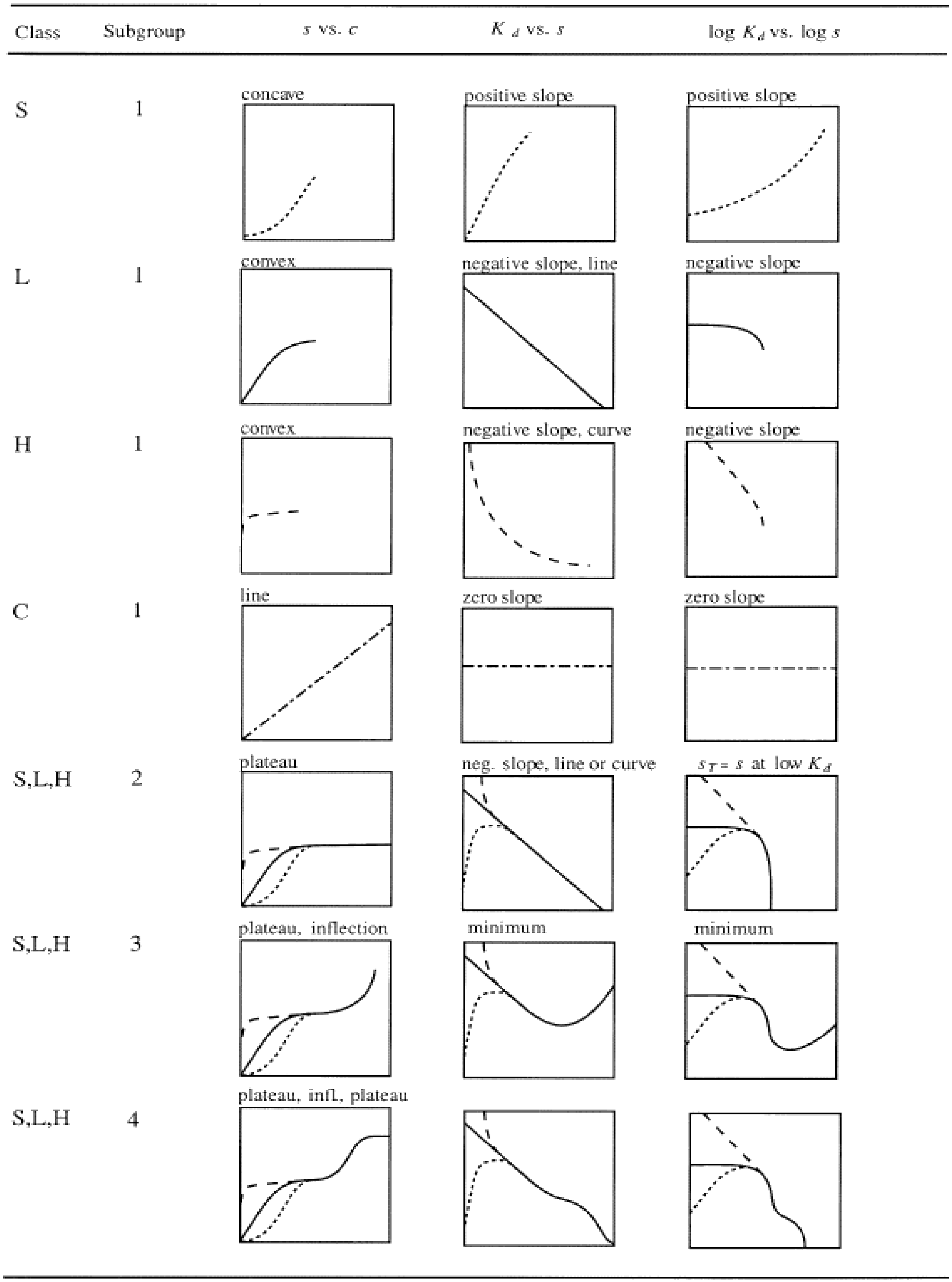

Figure 5. Isotherm classification according to Giles et al. (1974)[104].
Source: HINZ (2001)[105].

Adsorption isotherms are widely used to represent equilibrium states of an adsorption system. They are the first experimental information considered to choose between different adsorbents, since different materials produce biochars with different characteristics[83,19]. The adsorption isotherms indicate:

- How the adsorbent will effectively adsorb the solute;
- An estimate of the maximum amount of solute that the adsorbent will adsorb;

The experimental process carried out for the determination of the isotherms consists in placing the solution containing the component to be adsorbed with different masses of adsorbent (or a determined adsorbent mass may be used and varying the adsorbate concentrations) until equilibrium is reached. After filtration, the equilibrium concentration in the solution and the amount of adsorbate that has been adsorbed can be obtained, being possible to plot the isotherm[83,91].

2.8.1 Langmuir isotherm

The Langmuir isotherm is one of the first equations used to explain adsorption processes, mainly to describe monolayer adsorption processes[106]. The Langmuir isotherm is given in Equation 6.

$$Q_e = \frac{Q_m\, K_L\, C_e}{1 + K_L\, C_e} \tag{6}$$

where Q_e (mg g^{-1}) is the adsorbed concentration at equilibrium, Q_m (mg g^{-1}) is the maximum adsorption capacity after the formation of a monomolecular layer of the solute on the adsorbent surface, K_L (L g^{-1}) is the Langmuir coefficient, related to the affinity of the solute for the adsorbent and C_e (mg L^{-1}) is the concentration of the solute in the solution at equilibrium[107].

The Langmuir isotherm is based on the following assumptions[108]:

- The adsorption surface is homogeneous. In other words, the adsorption is constant and independent of the extension of the surface cover;
- Adsorption occurs at specific sites, without interaction with solute molecules;

- The adsorption becomes maximum when a monomolecular layer totally covers the adsorbent surface;
- The surface reveals a finite number of adsorption sites.

Bibaj et al. (2019)[109], evaluating the adsorption of nickel using banana peels as a source for activated carbon, obtained adsorption data that best fit the Langmuir model. Shukla & Pai (2005)[87] also obtained a better fit to the data using the Langmuir isotherm by evaluating the adsorption of Cu(II), Ni(II) and Zn(II) using activated carbons from jute (a vegetal fiber, which is basically cultivated in India and in Bangladesh).

2.8.2 Freundlich isotherm

The Freundlich model is used to evaluate the equilibrium conditions assuming a multi-molecular layer adsorption mechanism[110], different from the Langmuir model.

According to this model, the adsorption energy decreases logarithmically, as the surface is being covered by the adsorbate. When this is admitted to occur due to the heterogeneity of the surface, the Freundlich's model is no longer purely empirical. The nonlinear form of the equation is shown in Equation 7.

$$Q_e = K_f \, C_e^{\frac{1}{n}} \tag{7}$$

where Q_e (mg g^{-1}) is the amount of solute retained by the adsorbent, K_f is the Freundlich coefficient, an intercept that indicates the ability of the adsorbent to retain the solute, C_e (mg L^{-1}) is the solute concentration in the solution and n is a dimensionless parameter associated with the inclination of the isotherm[107]. Mathematically n can be interpreted as the measure of heterogeneity between the adsorption sites[111].

According to Awoyemi (2011)[112], the application of the model is limited to concentrations below saturation, where adsorption phenomena are not significant and still does not provide a limit of adsorption capacity, because with the increase of the adsorbed amount the concentration increases infinitely in this model. In the Freundlich isotherm, the presence of adsorbed ions in the neighboring sites of the adsorbent surface affects the adsorption of ions, causing steric hindrance and, therefore, the adsorption energy for each site is different[113].

2.8.3 Tóth isotherm

The Tóth model (TOTH, 1981)[114] was developed to modify the Langmuir equation in order to improve the fitting of the model to experimental data, and is often useful to describe heterogeneous systems[115]. Although the Tóth model is derived from gas/solid studies, the model can be extended to liquid/solid adsorption systems[116]. The general isotherm equation (GIE) form is shown in Equation 8.

$$Q_e = \frac{Q_m \cdot \alpha \cdot C_e^{m_a}}{1 + \alpha \cdot C_e^{m_a} - k \cdot C_e^{m_k}} \tag{8}$$

where Q_e (mg g^{-1}) is the adsorbed concentration, Q_m (mg g^{-1}) is the maximum adsorption capacity, C_e (mg L^{-1}) is the solute concentration in the solution, α, m_a, m_k and k are the isotherm constants.

Vijayaraghavan et al. (2006)[117], Brdar et al. (2012)[118] and Thi & Van (2016)[119] used the Tóth isotherm (not as GIE form) to describe the adsorptive process of heavy metals.

3 MATERIALS AND METHODS

3.1 Reagent and materials

Tangerine peels were obtained after domestic use. 97% iron (III) chloride hexahydrate ($FeCl_3 \cdot 6H_2O$) was supplied from Panreac, 95% nickel(II) chloride hexahydrate ($NiCl_2 \cdot 6H_2O$), 98% sodium hydroxide (NaOH) and 37% hydrochloric acid (HCl) were obtained from Fisher chemical. Nitrogen 99.995% was supplied from Praxair. Distilled water was used throughout the research.

3.2 Production of the activated carbons

Tangerine peels were firstly placed in oven at 100 ºC for 24 h in order to dry. Later they were grinded and sieved. For the production of activated carbons, the particle sizes between 106 and 250 µm were used and it was achieved using two sieves with metallic mesh (CISA) according to ISO 3310.1 and ASTM E-11-95 (Nº 140 and 60, respectively).

Activated carbons were prepared from the peels of tangerine in two steps: 1) hydrothermal activation and 2) pyrolysis. For the activation stage, 2.5 g of the dried sieved peels were immersed in 20 mL of $FeCl_3$ solution at different concentrations (2.5, 1.0 and 0.5 M) and kept in a 125 mL removable Teflon vessel inserted in a stainless high-pressure reactor (Model 249M 4744-49, Parr Instrument co., USA) under autogenous pressure at 200 ºC for 3 h (Figure 6A and Figure 6B).

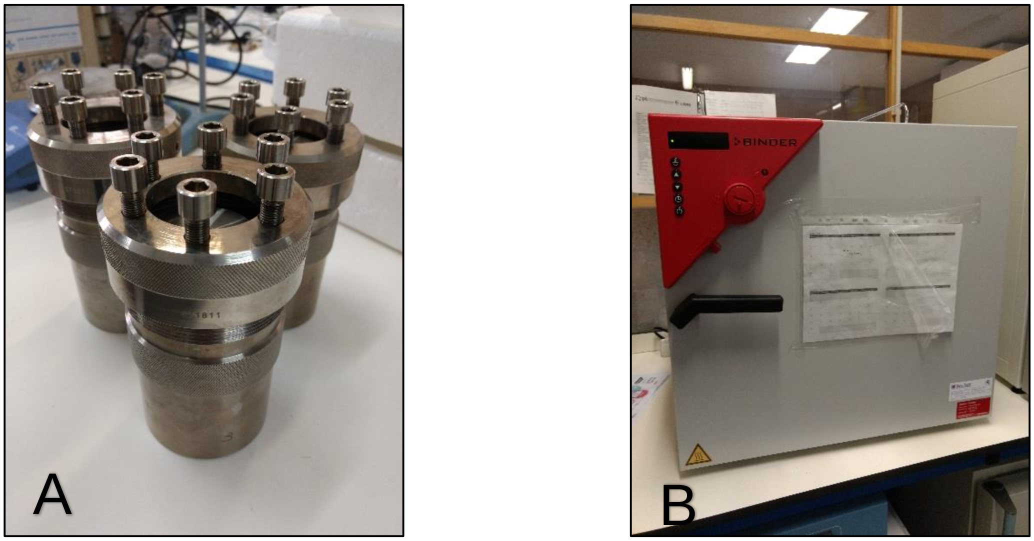

Figure 6. Stainless steel high-pressure batch reactor (A); Oven used in the activation process (B).

After cooling, the resultant suspension was filtered in order to recover the liquid and the solid fractions. The recovered solid was washed with distilled water several times until the rising waters reached the natural pH of distilled water and reveal absence of color. Then, the solid material was dried overnight in oven at 60 ºC. The liquid fraction was recovered to determine its TOC (Total Organic Carbon) in order to assess the carbon loss from the raw biomass.

The carbonization of the activated and of the non-activated samples was carried out under nitrogen continuous flow (100 cm^3 min^{-1}) at 800 ºC, for 4 h, using the tubular furnace (Therm Concept) shown in Figure 7.

Figure 7. Tubular furnace used in the pyrolysis process.

The prepared materials were named as follows:

- TW-C: Pyrolized tangerine peels.
- TW-Fe-0.5-C: Tangerine peels treated by HTC with $FeCl_3$ 0.5 M and pyrolysis.
- TW-Fe-1.0-C: Tangerine peels treated by HTC with $FeCl_3$ 1.0 M and pyrolysis.
- TW-Fe-2.5-C: Tangerine peels treated by HTC with $FeCl_3$ 2.5 M and pyrolysis.
- TW-Fe-2.5: Tangerine peels treated by HTC with $FeCl_3$ 2.5 M.

3.3 TOC of liquid fraction from HTC

The TOC quantification of the liquid samples taken from the HTC runs was performed using a Shimadzu TOC-L CSH/CSN equipment. To prepare the samples for analysis, a first dilution was made using 1 mL of the sample in a 250 mL volumetric flask, making up the rest with distilled water. The equipment to quantify TOC can be seen in Figure 8.

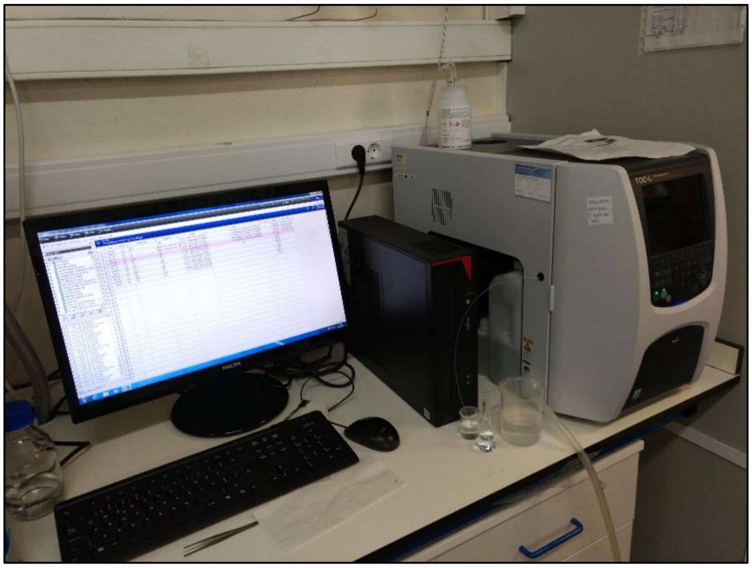

Figure 8. Equipment used for TOC analysis.

3.4 Burn-off

The degree of burn-off should be interpreted as the reduction in mass of the material after the pyrolysis process. Several authors still claim that higher burn-off rates and lower yields may be associated with improved textural properties of activated carbon[120,121,122,123,124]. The burn-off level was calculated using equation (9).

$$Burn-off\ (\%) = \frac{(m_i - m_f)}{m_i} * 100 \tag{9}$$

where m_i is the initial mass and m_f is the mass after the pyrolysis process.

3.5 Characterization of ACs

3.5.1 Ash content

To determine the ash content, a muffle (Figure 9) was used. First, the crucibles were calcined at 800 ºC for 30 minutes, then the empty crucible was weighed (P1), 0.1 g of activated carbon (P3) was added to the crucibles and taken to the muffle, where they remained for 4 h at 800 ºC. After that time, the crucibles were allowed to cool and were weighed with the calcined samples (P2). The ash content was calculated according to equation 10.

$$Ash\ (\%) = \frac{(P_2 - P_1)}{P_3} * 100 \tag{10}$$

Figure 9. Muffle used to determine ash content.

3.5.2 Elemental analysis

The composition of the materials were determined by elemental analysis (Carlo Erba Instrument EA 1108) to know the weight percentages of Carbon, Nitrogen, Hydrogen and Sulfur for both the raw biomass and the materials produced.

3.5.3 Surface chemistry analysis

To determine the acidity and basicity of the ACs it was applied an acid-base titration. First, 0.2 g of activated carbon were weighed and placed in contact with 25 mL of 0.02 mol L^{-1} sodium hydroxide (NaOH) and 0.02 mol L^{-1} hydrochloric acid (HCl) solutions in 100 mL flasks. The flasks with the solutions and the adsorbent were closed and shaken for 48 h, in a shaker at 320 rpm. Subsequently, the solutions were filtered and 20 mL of the NaOH and HCl solutions titrated with hydrochloric acid (HCl 0.02 mol L^{-1}) and sodium hydroxide solutions (NaOH 0.02 mol L^{-1}), respectively. The surface acidity and basicity on the carbons were calculated, in mmol g^{-1}, according to Equation 11.

$$Acidity\ /\ Basicity = \left(\frac{0.025}{m}\right) * \left(\frac{C_{ab} - (V_t * C_{tab})}{0.020}\right) \tag{11}$$

where m is the amount of carbon (g), C_{ab} is the concentration of NaOH or HCl in solution, V_t is the titrated volume of NaOH or HCl and C_{tab} is the concentration of NaOH or HCl for titration.

3.6 Ni(II) adsorption runs

3.6.1 Adsorption kinetics of Ni(II)

First, 0.25 g of activated carbon were placed in a 250 mL Erlenmeyer containing 100 mL of a 5 mg L^{-1} nickel(II) chloride solution at natural pH (around 6). The moment in which the activated carbon is placed was defined as the initial time $t_0 = 0$. The adsorption was promoted at 240 rpm and at 25 ºC using an incubator Shel Lab SI4 (Figure 10). Then, different samples were withdrawn from the Erlenmeyer at the following selected times: 15, 30, 60, 120, 240 and 1440 min. The samples were filtered in order to separate the adsorbent from the liquid fraction. Then, the Ni(II) ions were quantitatively analyzed by atomic absorption spectrophotometry.

Figure 10. Incubator used for analysis.

The amount of nickel adsorbed on the activated carbon in each test was calculated using the previously defined Equation 1.

3.6.2 Equilibrium adsorption isotherms of Ni(II)

The adsorption was studied by means of the equilibrium method. First, 0.125 g of activated carbon were placed in a 250 mL Erlenmeyer containing 50 mL of the nickel(II) chloride hexahydrate solution, at different concentrations (0, 10, 20, 50, 80, 100, 250, 750 and 1000 mg L^{-1}) and under the pH of the solution (around 6). The mixtures were stirred at 240 rpm for 72 h at room temperature (25 ºC). Samples were filtered and analyzed, as above explained.

After obtaining the data, modeling was performed to identify which isotherm best represented the adsorption process.

3.6.3 Study of pH effect on the removal of Ni(II) by activated carbon

The pH values of the Ni(II) solution studied were 3, 5, 7 and 9. For each run, 25 mL of the 100 mg L^{-1} nickel(II) chloride hexahydrate was used with 0.0625 g of the adsorbent (2.5 g L^{-1}) and a contact time of 72 h. The pH of the solution was adjusted using 1 mol L^{-1} HCl and 1 mol L^{-1} NaOH during all runs. After 72 h, the samples were filtered in order to separate the adsorbent from the liquid fraction and the concentration of Ni (II) in the filtrate was determined.

3.6.4 Determination of nickel

The concentrations of Ni(II) in the filtrates obtained in the experimental runs were obtained by atomic absorption spectroscopy in a Varian SpectrAA 220 (Varian, Steinhausen, Switzerland).

3.7 Modelling and statistical methods

Kinetic and isotherm models were fitted by non-linear analysis in order to avoid errors generated by different estimates resulting from the simple linear regression of the linearized forms. This provides a mathematically rigorous method for determining isothermal parameters using the original form of the isothermal equation[125,126]. The adsorption equilibrium data for nickel were analyzed by non-linear curve fitting analysis, using software OriginPro 8.5. For analysis and validation of kinetic models, adsorption isotherms and their parameters, the t-test and the F-test with a 5% significance level (α_{prob}) were used. The kinetic mechanism controlling the adsorption process were evaluated fitting the pseudo-first order (Equation 3), the pseudo-second order (Equation 4) and the Elovich (Equation 5) models by non-linear regression. To evaluate the Langmuir, Freundlich and the GIE of Tóth, equations 6, 7 and 8 were used, respectively. The sets of isothermal parameters were determined by non-linear regression.

The student's t-test was used to analyze the null hypothesis that the calculated parameter value is zero. The higher the t value, the lower the probability of the analyzed parameter to be zero, however the Prob. > |t| is easier to interpret, since this, being less than α_{prob} means that we can reject the null hypothesis of the t-test and assume that the calculated parameter is significant. The smaller Prob. > |t|, the more unlikely the parameter is equal to zero[127].

The Fisher's F-test was used in the regression analysis to test the hypothesis that all model parameters are zero. The F Value and Prob. > F statistics test the overall significance of the regression model. Regarding the F value, it can be inferred that the higher is the deviation of this parameter from 1, the stronger is the evidence that the adjusted model differs significantly from the null hypothesis. If Prob. > F is less than α_{prob}, it can be concluded that the model has statistical significance[127].

A parity graph was used to assess the final adjust of the calculated values in relation to the experimental data. Each point has coordinates (x, y), where x is the calculated value and y is the corresponding experimental value. A line of the equation y = x is drawn as a reference, when an experimental value is close to a calculated value, the closer these points are to the line y = x[128].

4 RESULTS AND DISCUSSION

4.1 Preparation of activated carbons: burn-off and TOC

The activated carbons were prepared according to the procedure described in the experimental section. The precursor and the resultant solid material obtained after the pyrolysis process was weighted to determine burn-off. The liquid phase of the samples prepared by HTC was collected to analyze the values of TOC. In this way, it is possible to confirm the amount of organic carbon that was lost during the hydrothermal carbonization process. Table 6 shows the burn-off levels obtained for the activated carbon that underwent the pyrolysis process, as well as the TOC values obtained in the liquid phase of the HTC process.

Table 6. Burn-off levels and TOC obtained in the HTC and pyrolysis process.

AC	**Burn-off (wt%)**	**TOC (g L^{-1})**
TW-C	76.40	--
TW-Fe-0.5-C	52.60	17.70
TW-Fe-1.0-C	50.95	18.80
TW-Fe-2.5-C	48.97	11.50
TW-Fe-2.5	--	11.50

According to Teng and Lin (1998)[122] the surface area and the pore volume of the activated carbons increase with the increase in the temperature of pyrolysis and the proportion of volume of micro, mesopores and the average diameter of the pores generally increases with the level of burn-off.

From Table 6, it is possible to observe that the activated carbon that did not go through the HTC process, and therefore did not contain iron in its composition, had the highest burn-off level in the pyrolysis (76.40%). Lim et al. (2010)[129], evaluating the yields of activated carbons obtained from palm shells using phosphoric acid as an activating agent, justified that lower burn-off values were obtained due to the presence of phosphoric acid. It was explained due to the capacity to form a bond layer, such as esters of phosphate and polyphosphate, which can protect the structure of the internal pores and thus prevent the adsorbent from excessive burning. The same reasoning can be applied in the results obtained in this work, considering that when modifying the activated carbons with iron, the surface chemistry of the carbon changes due to modification of the functional groups[130].

Liu et al. (2018)[131], evaluating the effects of $FeCl_3$ (impregnation with $FeCl_3$ and subsequent pyrolysis at 800 ºC) on the physico-chemical structure of activated carbons obtained from Jixi bituminous coal observed that, as the amount of $FeCl_3$ increased, the volume of micropores increased, indicating an increase in the quantity and in the presence of larger micropores. The authors still state that these changes may be related to the catalytic cracking characteristics of $FeCl_3$[132]. According to Gong et al. (2009)[133], the addition of iron-based catalysts caused the cleavage of microcrystalline structure, releasing volatile matter (such as CO or CO_2) and leading to the formation of pores.

This fact can also be used to justify the concentrations of organic carbon found in the liquid phase of the prepared samples. Release of organic matter present in the tangerine peels as a result of the action of the activating agent. It was expected that activated carbon with a higher concentration of $FeCl_3$ would have a higher concentration of organic matter in solution, a fact that was not observed. The activated carbon TW-Fe-1.0-C had the highest TOC (18.80 g L^{-1}).

4.2 Characterization of activated carbons

4.2.1 Elemental composition and ash content

Table 7 shows the values of carbon, hydrogen, nitrogen, sulfur and ash for the tangerine peels and for the activated carbons prepared.

Table 7. Elemental composition and ash content in the tangerine peels and in the activated carbons.

Sample	C (%)	H (%)	N (%)	S (%)	Non-identified[1] (%)	C/H	Ash (%)
Peels	42.1 ± 0.1	6.17 ± 0.03	0.77 ± 0.05	0.05 ± 0.03	46.46	6.82	4.4 ± 1.4
TW-C	79.4 ± 0.4	1.39 ± 0.02	1.63 ± 0.01	0.03 ± 0.01	9.55	57.2	8.0 ± 0.4
TW-Fe-0.5-C	93.1 ± 0.2	1.21 ± 0.04	1.01 ± 0.05	0.03 ± 0.02	2.45	77.0	2.2 ± 0.3
TW-Fe-1.0-C	90.8 ± 1.0	1.20 ± 0.00	0.86 ± 0.02	0.04 ± 0.01	3.80	75.8	3.3 ± 1.0
TW-Fe-2.5-C	87.6 ± 1.5	1.06 ± 0.03	0.02 ± 0.01	0.03 ± 0.03	6.21	82.8	5.1 ± 0.6
TW-Fe-2.5	65.9 ± 0.2	4.74 ± 0.05	0.44 ± 0.02	0.03 ± 0.01	24.04	13.9	4.8 ± 2.2

Note[1]: Obtained by the difference: 100%-C(%)-H(%)-N(%)-S(%)-Ash(%).

Comparing to the raw waste it is possible to observe that the carbon content increases and the hydrogen levels decrease. The pyrolysis process causes the release of volatile compounds, such as water and low molecular weight hydrocarbons[134,135]. Higher levels of hydrogen in carbon TW-Fe-2.5 occur due to the hydration process.

The C/H ratio has been accepted as an indication of condensation reactions or polycyclization reactions, common in the carbonization and activation process[136]. It can be seen that the C/H ratio increases during pyrolysis or HTC, since all materials show higher C/H ratio when compared to the raw materials (6.82). This is a typical result of any carbonization process, since it is known that it improves the aromaticity of the original waste[135]. ACs prepared by sequential HTC and pyrolysis show a higher C/H ratio (77.0-82.8) when compared to the material prepared only by pyrolysis (57.2) or by HTC (13.9). Among them, Sample TW-Fe-2.5-C had the highest C/H ratio, being slightly more than 12 times greater than that of tangerine peels.

After pyrolysis, an increment of the ash content of the solid material is expected by the volatilization of part of the organic compounds of the raw material, as observed in the material TW-C (8.0%). However, HTC leads to decrease the ash content up to 2.2%, likely because the iron chloride solution causes the dissolution of some inorganic compounds of the raw material. The ash content of an activated carbon is a measure of the inert, inorganic, and unusable part of the material and their presence in activated carbon is harmful in the adsorption process, since they modify the interaction between the surface of the activated carbon and the substance to be adsorbed[137]. The ash content increases by rising the iron chloride concentration, due to iron incorporation.

Non-identified species (different from C, H, N, S and ashes) is typically associated to the element oxygen. As observed, its content decreases after either pyrolysis or HTC, as a consequence of the carbonization processes (oxygen is released). Fernandez et al. (2015)[62] evaluating the adsorbent potential of activated carbons prepared from orange peels also observed an increase in carbon content after hydrochar pyrolysis, as well as a reduction in the H content due to the dehydration process.

4.2.2 Surface acidity and basicity

Agricultural residues are generally composed of lignin, cellulose and hemicellulose. Being the main chemical components contained in these residues, they present a variety of functional groups[36].

The adsorptive properties of ACs are influenced not only by its textural properties, such as porosity and surface area, but the surface chemistry also has a strong effect[138]. The functional groups present at the surface of activated carbons may contain heteroatoms such as oxygen, nitrogen and phosphorus that form organic functional groups, such as carbonyls, carboxylic acids, lactones, ethers, phenols, aldehydes, amines and phosphates, which can be neutral, acidic or basic. The surface chemistry depends on the composition of the raw material used and on the activation method[139,140]. The results obtained in terms of acidity and basicity of the activated carbons prepared are shown in Table 8.

Table 8. Acidity and basicity of activated carbons prepared.

AC	**Acidity (mmol g^{-1})**	**Basicity (mmol g^{-1})**
TW-C	0.00	1.83
TW-Fe-0.5-C	0.15	0.63
TW-Fe-1.0-C	0.04	0.88
TW-Fe-2.5-C	0.23	0.70
TW-Fe-2.5	N.A.*	0.21

* N.A. = Not applied.

As observed, the activated carbons prepared by HTC, when compared to the biochar, prepared only by pyrolysis (TW-C), show changes in the total acidity and total basicity of the activated samples.

According to the data given in Table 8, it can be seen that the content of acid groups in sample TW-Fe-2.5-C is the highest among all the analyzed samples. On the other hand, sample TW-C has a larger number of basic sites when compared to the other samples and no acidic sites were identified. Less basicity in the ACs prepared by HTC could be ascribed to the chloride precursor used as activating agent.

Largitte et al. (2016)[141], when assessing the adsorption of lead in aqueous medium using activated carbons prepared from guava seeds and almond shells (lignocellulosic residues), observed that the activated carbon prepared from almond shells showed only alkaline groups on its surface and pointed out that the ion exchange mechanism must occur with a static interaction of the cation Pb^{2+} and the π-electrons present in the graphene layer of the carbon, while the activated carbons that have acid groups will favor the ion exchange mechanism with the surface groups of these carbons.

Acid behavior is associated with surface oxygen complexes or oxygen functionalities, such as carboxyls, lactones and phenols. On the other hand, functionalities such as pyrones, chromenes, ethers and carbonyls are responsible for the basic properties of carbon surfaces[139,142]. Menéndez et al. (1996)[143] associate the basicity of activated carbons to the absence of oxygen-containing groups that are predominantly acidic in nature.

4.3 Nickel adsorption

4.3.1 Adsorption kinetics

Table 9 summarizes the results obtained for the amount of nickel adsorbed on all materials at equilibrium (Q_e) during the adsorption runs.

Table 9. Amount of Ni(II) adsorbed at natural pH, room temperature and 2.5 g L^{-1} of adsorbent after 72 h.

Initial concentration of Ni (II) (mg L^{-1})	Amount adsorbed, *Qe* (mg g^{-1})				
	TW-C	TW-Fe-0.5-C	TW-Fe-1.0-C	TW-Fe-2.5-C	TW-Fe-2.5
10	3.98	0.83	3.32	2.87	2.03
20	7.76	1.53	1.93	4.11	2.08
50	11.17	0.10	2.16	5.17	2.68
80	13.90	N.A.*	4.10	5.18	3.97
100	13.95	2.00	5.48	5.00	2.91
250	15.74	N.A.*	N.A.*	12.34	N.A.*
750	37.89	N.A.*	N.A.*	19.75	N.A.*
1000	50.16	4.50	N.A.*	28.75	N.A.*

* N.A. = Not applied.

It should be emphasized that the concentrations of 250 and 750 mg L^{-1} were only considered for the samples TW-C and TW-Fe-2.5-C, those showing the best results, so it was done to guarantee a better fittings of the isotherm and kinetic models to the results.

The kinetic adsorption data were modeled using kinetic equations of pseudo-first order (3), pseudo-second order (4) and Elovich (5) to get insights about the adsorption mechanism. The kinetic models for Ni(II) adsorption are displayed in Figure 11 and Figure 12, and the results for the kinetic parameters, Prob. > |t|, Prob. > F, F Value and correlation coefficients (R^2), are listed in Table 10. In Table 11 are showed the amount of substance adsorbed at time t (Q_t) and removal percentage.

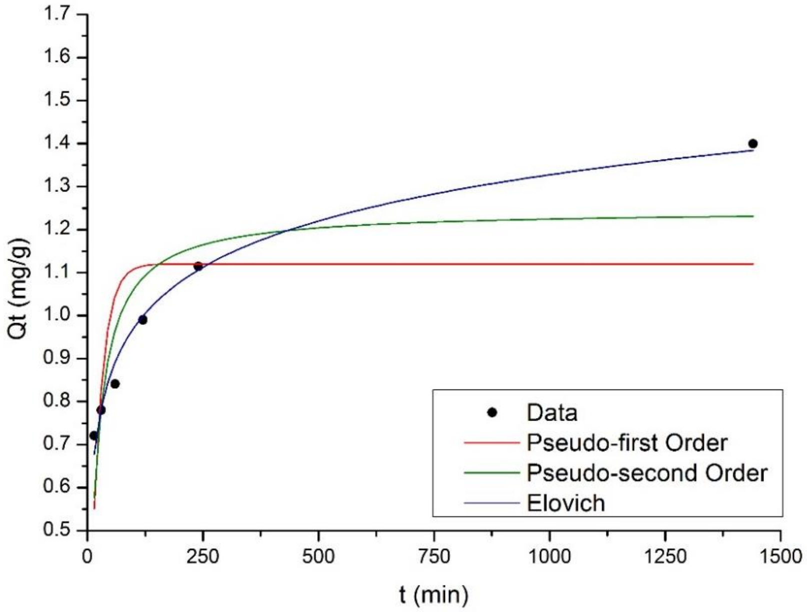

Figure 11. Modelling of the amount of Ni(II) adsorbed as a function of time for the activated carbon TW-C (2.5 g L^{-1}) at 25 ºC, C_0 = 5 mg L^{-1} and pH 6.

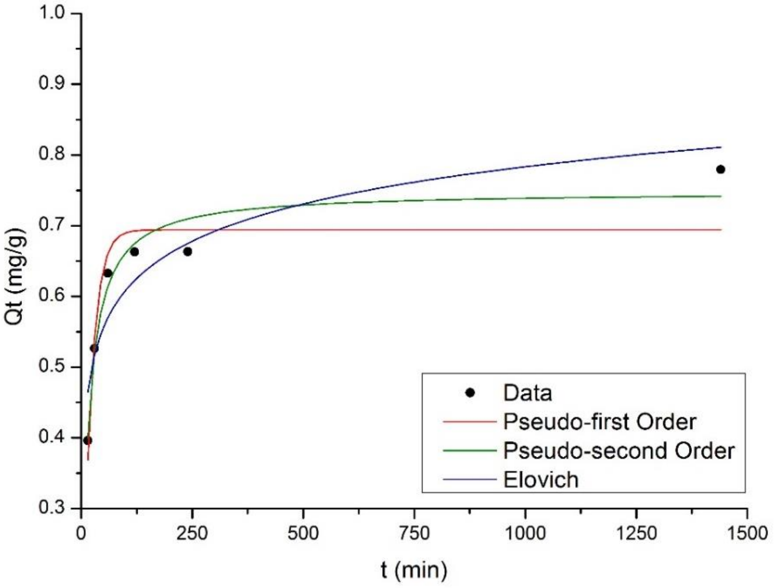

Figure 12. Modelling of the amount of Ni(II) adsorbed as a function of time for the activated carbon TW-Fe-2.5-C (2.5 g L^{-1}) at 25 ºC, C_0 = 5 mg L^{-1} and pH 6.

Table 10. Kinetic parameters for adsorption of Ni(II) onto the activated carbons TW-C and TW-Fe-2.5-C, at 25 °C.

AC	**Pseudo-first Order**					
	Parameter		**Prob. > │t│**	**Prob. > F**	**F Value**	**R²**
TW-C	**Q_e (mg g^{-1})**	1.120	5.87E-04	0.0011	70.062	0.479
	K_1 (min^{-1})	0.0452	0.0752			
TW-Fe-2.5-C	**Q_e (mg g^{-1})**	0.6944	1.64E-05	3.28E-05	424.25	0.876
	K_1 (min^{-1})	0.0505	0.0048			
	Pseudo-second Order					
TW-C	**Q_e (mg g^{-1})**	1.246	2.51E-04	2.39E-04	155.015	0.761
	K_2 (g mg^{-1} min^{-1})	0.0462	0.0942			
TW-Fe-2.5-C	**Q_e (mg g^{-1})**	0.7483	4.74E-06	4.73E-06	1,123.023	0.953
	K_2 (g mg^{-1} min^{-1})	0.1020	0.0058			
	Elovich					
TW-C	**α (mg g^{-1} min^{-1})**	0.8106	0.0440	9.43E-07	2,519.01	0.985
	β (g mg^{-1})	6.450	9.02E-05			
TW-Fe-2.5-C	**α (mg g^{-1} min^{-1})**	2.313	0.5176	3.68E-05	400.658	0.868
	β (g mg^{-1})	13.181	0.0070			

Note[1]: If “Prob. > |t|” < α_{prob} (0.05) the calculated parameter has statistical significance.
Note[2]: If “Prob. > F” < α_{prob} (0.05) the model has statistical significance.
Note[3]: The further this parameter deviates from 1, the stronger the evidence that the model has statistical significance.

Table 11. Amount of substance adsorbed at time t (Q_t) and removal percentage.

Time (min)	Q_t (mg g^{-1})	Removal %	Q_t (mg g^{-1})	Removal %
	TW-C		**TW-Fe-2.5-C**	
15	0.72	36.02	0.40	19.80
30	0.78	39.00	0.53	26.32
60	0.84	42.04	0.63	31.64
120	0.99	49.48	0.66	33.14
240	1.11	55.70	0.66	33.16
480	1.31	65.72	0.65	32.60
1440	1.40	69.96	0.78	38.98

As observed in Table 11, the AC TW-C shows a greater adsorption capacity of Ni(II). The adsorption kinetics makes it possible to visualize that after 1 h of the beginning of the process just over 42% of the nickel has been adsorbed and at the end of the process, 70% of the Ni(II) has been removed from the aqueous medium. For the AC TW-Fe-2.5-C, at the end of the process almost 40% of the Ni(II) has been adsorbed. It is necessary to emphasize again the crucial role of pH in adsorptive processes that are favored in more basic values.

As shown in Table 10, the model that best describes the adsorptive process of nickel with the activated carbon TW-C is Elovich with an R^2 of 0.9851 and a Prob. > F below the 5% established as a significance interval, as well as its two parameters (α and β) showing statistical significance. The AC TW-Fe-2.5-C, on the other hand, despite the Elovich model showing statistical significance according to F-test, its α parameter presented Prob. > |t| higher than that established by the significance interval, being therefore rejected. Therefore, the pseudo-second order model describes better the process. With the parity graphs presented below (Figure 13), it is possible to visualize more clearly the models that best describes the experimental data.

Kumar et al. (2010)[144], studying the adsorption of nickel in cashew nut shells, used the models of pseudo-first order, pseudo-second order and Elovich to evaluate the adsorptive process. The authors also observed that the model that best described the process was the pseudo-second order.

Sudha et al. (2015)[56] used the pseudo-first and pseudo-second order models to evaluate the lead(II) adsorption process using ACs prepared from Persia lime peels

(Citrus limettioides). The authors found that the pseudo-second order model was the most appropriate to describe the data.

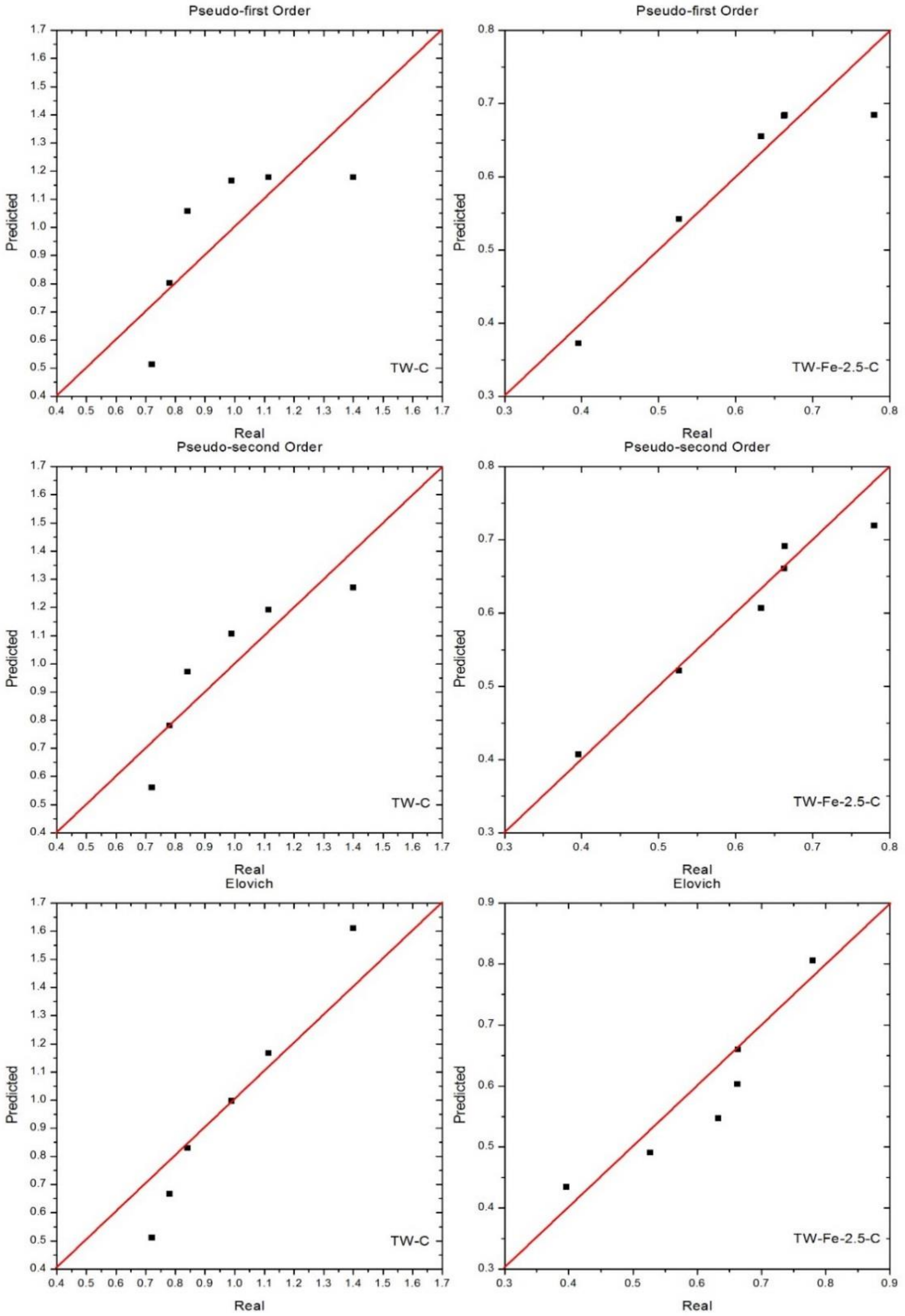

Figure 13. Parity graphs for the amount of nickel adsorbed at time *t* (Q_t) according to the kinetic models applied.

4.3.2 Equilibrium adsorption isotherms

The adsorption isotherms for the carbons TW-C and TW-Fe-2.5-C are shown in Figure 14 and Figure 15.

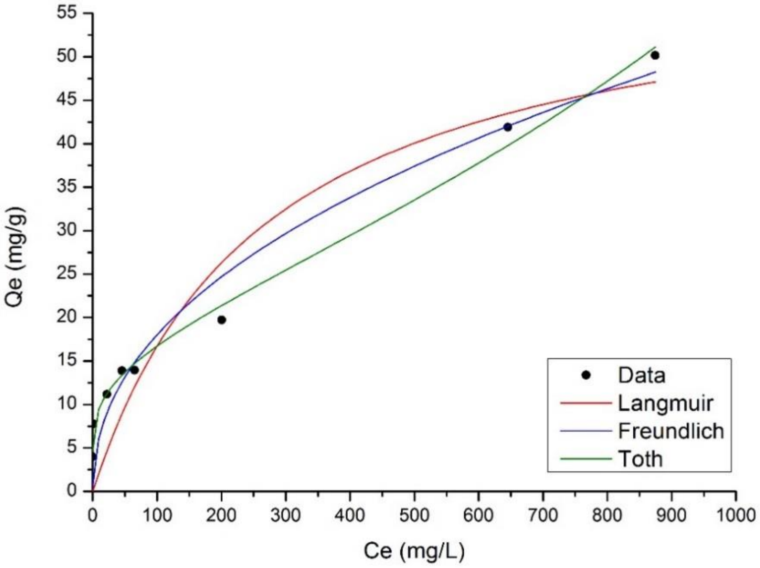

Figure 14. Adsorption isotherms for Ni(II) with activated carbon TW-C at natural pH, room temperature and 2.5 g/L of adsorbent after 72 h.

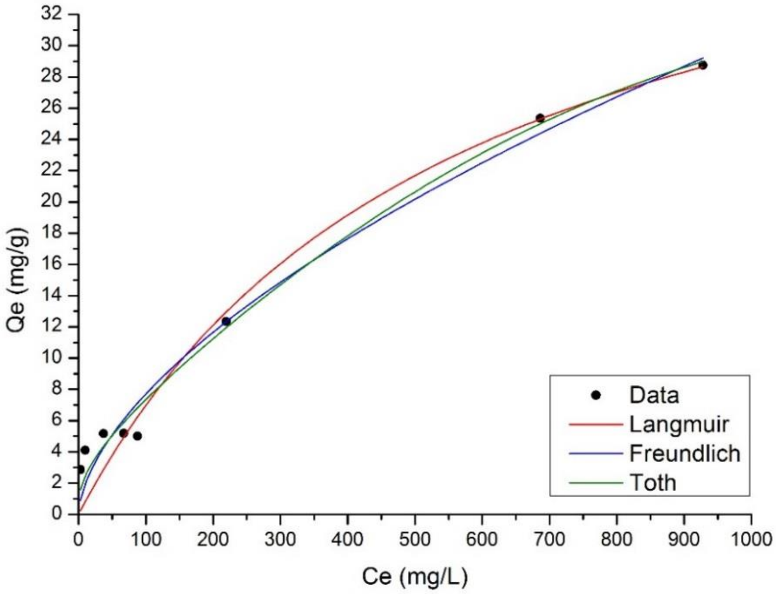

Figure 15. Adsorption isotherms for Ni(II) with activated carbon TW-Fe-2.5-C at natural pH, room temperature and 2.5 g/L of adsorbent after 72 h.

As it is possible to verify, the sample TW-C was more effective in removing nickel from the solution than TW-Fe-2.5-C. According to the surface chemistry analysis, the sample TW-Fe-2.5-C presents the highest amount of acidic sites, which would favor the removal of the heavy metal[145]. Furthermore, according to Liu et al. (2018)[131], the activating agent used ($FeCl_3$) has catalytic cracking characteristics, which would favor the creation of micropores.

However, Oliveira et al. (2008)[146], when preparing activated carbons made from coffee husks and activated with $FeCl_3$, emphasized that the removal of iron species is extremely important, since it avoids the blockage of pores and, consequently, a decrease in the adsorption capacity of adsorbents produced after activation with Fe salts. In Table 12 is shown the parameters calculated by nonlinear regression of the Langmuir, Freundlich and Tóth isotherms.

Table 12. Isotherm constants for the adsorption of Ni(II) by TW-C and TW-Fe-2.5-C at 25 ºC.

AC	**Langmuir**					
	Parameter		**Prob. > |t|**[1]	**Prob. > F**[2]	**F Value**[3]	**R**[2]
TW-C	**Q_m (mg g^{-1})**	61.5628	0.0018	1.27E-04	75.6676	0.8971
	K_L (L g^{-1})	0.0037	0.1006			
TW-Fe-2.5-C	**Q_m (mg g^{-1})**	45.7982	0.0013	7.61E-06	201.7895	0.9658
	K_L (L g^{-1})	0.0018	0.0368			
	Freundlich					
TW-C	**K_f (L^n g^{-n})**	2.2261	0.0336	9.48E-06	187.1564	0.9574
	n	2.2023	2.44E-04			
TW-Fe-2.5-C	**K_f (L^n g^{-n})**	0.1715	0.0289	1.91E-06	323.0605	0.9785
	n	1.6718	3.55E-05			
	Tóth					
TW-C	**Q_m (mg g^{-1})**	79.9539	0.9961	3.67E-04	268.4372	0.9939
	α (L^{m_a} g$^{-m_a}$)	0.0045	0.9964			
	m_a	0.0122	0.9484			
	m_k	0.0071	0.9599			
	K (L^{m_k} g$^{-m_k}$)	0.9504	1.31E-06			
TW-Fe-2.5-C	**Q_m (mg g^{-1})**	8.1413	0.9926	0.00215	81.8098	0.9830
	α (L^{m_a} g$^{-m_a}$)	0.0097	0.9935			
	m_a	0.2382	0.9463			
	m_k	0.0168	0.9798			
	K (L^{m_k} g$^{-m_k}$)	0.9236	0.0026			

Note[1]: If "Prob. > |t|" < α_{prob} (0.05) the calculated parameter has statistical significance.
Note[2]: If "Prob. > F" < α_{prob} (0.05) the model has statistical significance.
Note[3]: The further this parameter deviates from 1, the stronger the evidence that the model has statistical significance.

As shown in Table 12, according to the R^2 value, the Tóth model was that one best describing the experimental data. However, when the results of the t-test are evaluated, it appears that the parameters Q_m, a, m_a and m_k did not show statistical significance in the 5% confidence level. On the other hand, the Freundlich model was able to describe the experimental data with certain precision, with a R^2 of 0.9557 for TW-C and 0.9785 for TW-Fe-2.5-C and the two parameters of the equation (K_f and n) were capable of presenting statistical significance.

The fittings of the models to the experimental data can be better visualized in the parity graphs given with the experimental data and predicted values for the amount of nickel adsorbed in the equilibrium (Q_e) (Figure 16).

Thi & Van (2016)[119], studying the adsorption of lead(II) using coffee husks, also obtained a better fit to the experimental data from the Toth model. However, the Freundlich model had the least average relative error (ARE), 0.85%, against 3.97% with the Tóth model, placing in evidence that the Freundlich model shows the best fit of the isotherm under the conditions of the experiment.

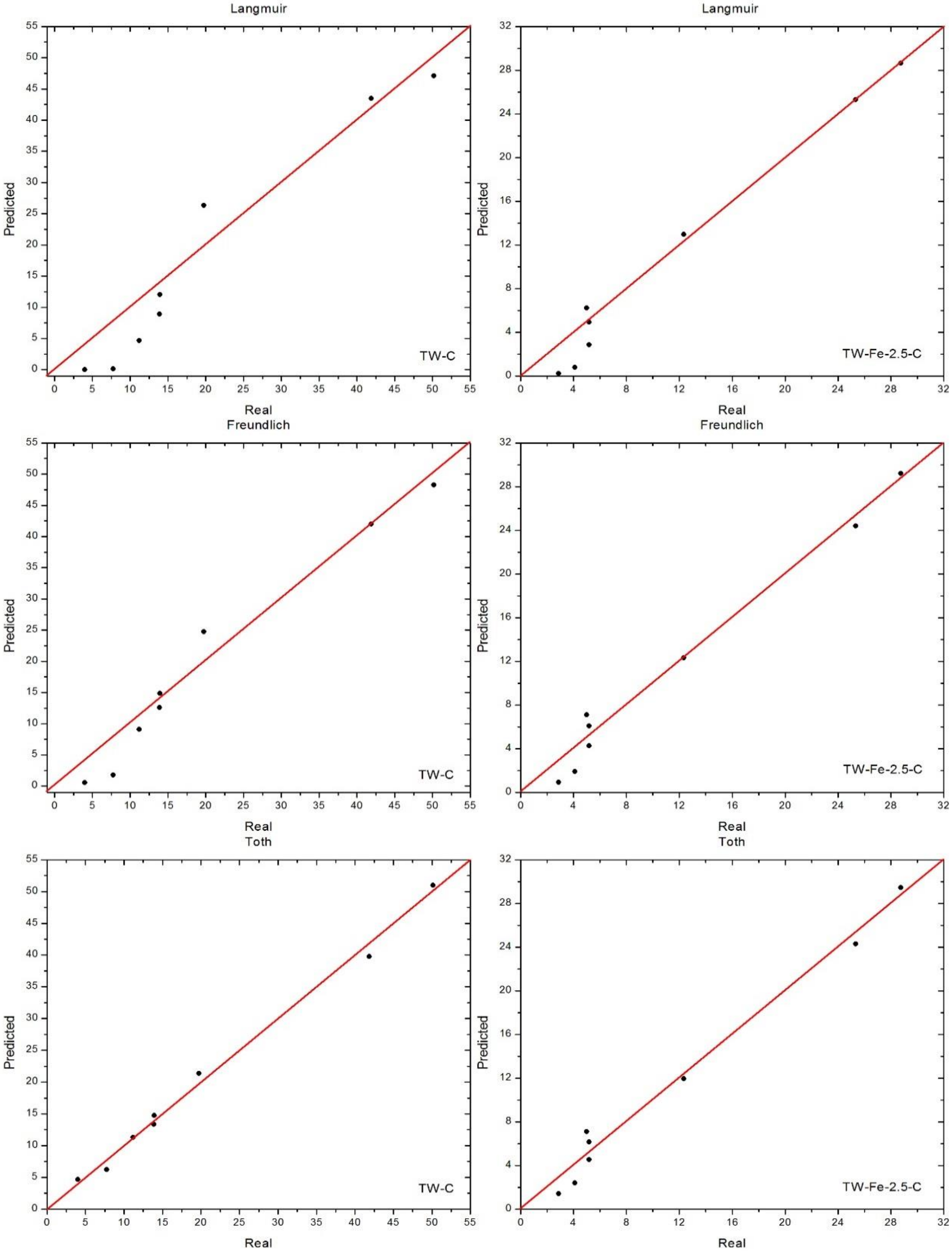

Figure 16. Parity graphs for the amount of nickel adsorbed (Q_e) according to the applied isotherms.

4.3.3 Effect of pH

pH plays a key role in the process of adsorption of heavy metals. This applies particularly to tangerine peel, an adsorbent of natural origin whose surface contains numerous acidic and basic functional groups, as above mentioned. The manipulation of the pH of the system can cause dissociation of these groups and cause a significant improvement or worsening of the efficiency of removal of Ni(II) ions. In Figure 17 and Table 13 is shown the effect of pH on nickel adsorption with the activated carbons evaluated.

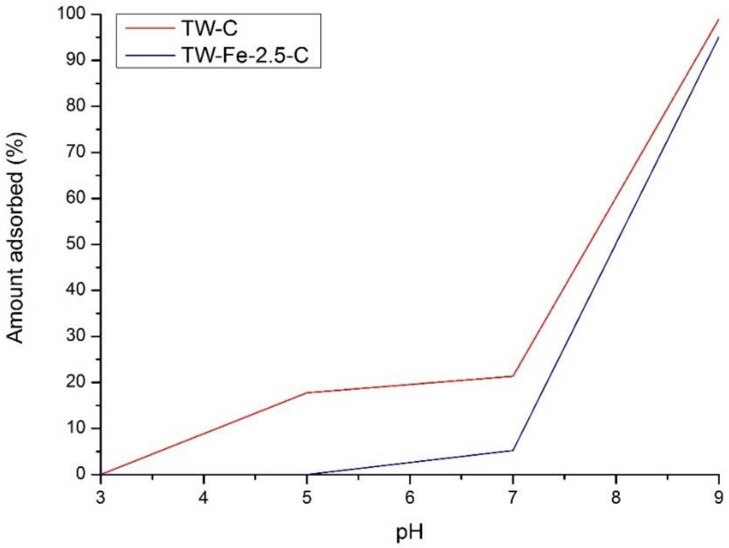

Figure 17. Effect of pH on the removal of Ni(II) ions with TW-C and TW-Fe-2.5-C at 25 ºC and C_0 = 100 mg L^{-1}.

Table 13. Experimental data from removal of Ni(II) ions with TW-C and TW-Fe-2.5-C at 25 ºC and C_0 = 100 mg L^{-1}.

pH	Ce (mg L^{-1})	Qe (mg g^{-1})	Amount adsorbed %
TW-C			
3	100.00	0.00	0.00
5	82.22	7.11	17.78
7	78.63	8.55	21.37
9	0.99	39.60	99.01
TW-Fe-2.5-C			
3	100.00	0.00	0.00
5	100.00	0.00	0.00
7	94.78	2.09	5.22
9	4.88	38.05	95.12

It is notable that at basic pH there is an increase in heavy metal adsorption, as reported by several authors. At pH 9, as shown in Figure 17, carbon TW-C adsorbed 99.01% of the heavy metal, while carbon TW-Fe-2.5-C adsorbed 95.12%. At pH 3 there was no adsorption for both carbons.

The adsorption of metal cations is improved at a higher pH, due to the lower number of H^+ ions, while at low pH there is a competition between hydronium cations and metals, reducing the adsorption of metal ions[36,86,87,147]. When the pH is higher, the concentration of H_3O^+ ions decreases and the sites on the surface of the carbon turn mainly into dissociated forms and can exchange H_3O^+ ions with metal ions in solution[148]. Bartczak et al. (2015)[77], evaluating the adsorption of nickel in aqueous medium using peat, also observed higher nickel adsorption at pH 9 (92.5%).

5 CONCLUSIONS

As shown, the carbons produced were able to remove nickel in aqueous solution. In topic 4.3.1, where the results obtained in the kinetic adsorption test are presented, it was possible to verify that carbon TW-C was more efficient in removing the heavy metal (69.96%), while carbon TW-Fe-2.5-C was able to remove 38.98%.

The application of ferric chloride as an activating agent, e.g. carbon TW-Fe-2.5-C lead to materials with lower efficiency than the carbon material without chemical activation (TW-C). As mentioned in section 4.3.2, this fact can be explained by the low removal of iron ions present in the carbon, which are able to block its pores and cause a reduction in its removal efficiency.

It should be noted that in order to better evaluate the efficiency of these activated carbons, it is necessary to take into consideration the textural properties (pore volume and surface area), as they have a direct influence on the adsorptive process. Moreover, it is important to carry out the kinetic tests under different conditions, varying the pH and the concentration of carbon in the solution, as these are factors that also influence the removal efficiency of the heavy metal.

Regarding the adsorption isotherms, according to statistical analysis, the Freundlich model was the one that managed to describe the experimental data in a more assertive way. The models presented R^2 of 0.9574 (TW-Fe-2.5-C) and 0.9785 (TW-C).

The pH of the solution proved to be one of the parameters that most influences the removal of heavy metals. As presented in topic 4.3.3, at more basic pH the adsorption process was favored due to the lower concentration of H_3O^+ and H^+ ions. At pH 9, the activated carbon TW-C was able to remove 99% of the nickel in solution, while the TW-Fe-2.5-C removed 95.1% of the metal.

Finally, from an economic point of view, it is interesting to carry out analyzes of activated carbon regeneration, not only for the reuse of activated carbon making the treatment process less costly, but also to recover the adsorbate for its reuse.

REFERENCES

1. Bhatti, H. N., Zaman, Q., Kausar, A., Noreen, S. & Iqbal, M. Efficient remediation of Zr(IV) using citrus peel waste biomass: kinetic, equilibrium and thermodynamic studies. *Ecol. Eng.* **95,** 216–228 (2016).

2. Jain, M., Garg, V. K. & Kadirvelu, K. Removal of Ni(II) from aqueous system by chemically modified sunflower biomass. *Desalin. Water Treat.* **52,** 5681–5695 (2014).

3. Rzetala, M. A. Assessment of toxic metal contamination of bottom sediments in water bodies in urban areas. *Soil Sediment Contam.* **24,** 49–63 (2015).

4. Kasprzak, K. S., Sunderman, F. W. & Salnikow, K. Nickel carcinogenesis. *Mutat. Res. - Fundam. Mol. Mech. Mutagen.* **533,** 67–97 (2003).

5. Shrestha, R. M., Varga, M., Varga, I., Yadav, A. P., Pokharel, B. P. & Pradhananga, R. R. Removal of Ni (II) from aqueous solution by adsorption onto activated carbon prepared from lapsi (Choerospondias axillaris) seed stone. *J. Inst. Eng.* **9,** 166–174 (2014).

6. Yu, J., Zhang, J., Song, S., Liu, H., Guo, Z. & Zhang, C. Removal of Ni(II) from aqueous solutions using activated carbon with manganese formate hydrate in-situ modification. *Colloids Surfaces A Physicochem. Eng. Asp.* **560,** 84–91 (2019).

7. Long, J., Huang, X., Fan, X., Peng, Y. & Xia, J. Effective adsorption of nickel (II) with Ulva lactuca dried biomass: Isotherms, kinetics and mechanisms. *Water Sci. Technol.* **78,** 156–164 (2018).

8. Malkoc, E. & Nuhoglu, Y. Investigations of nickel(II) removal from aqueous solutions using tea factory waste. *J. Hazard. Mater.* **127,** 120–128 (2005).

9. Meena, A. K., Mishra, G. K., Rai, P. K., Rajagopal, C. & Nagar, P. N. Removal of heavy metal ions from aqueous solutions using carbon aerogel as an adsorbent. *J. Hazard. Mater.* **122,** 161–170 (2005).

10. Beliles, R. P. in *Toxic. heavy Met. Environ.* (ed. Dekker, M.) 383 (F. W. Oehme, 1979).

11. Ates, N. & Uzal, N. Removal of heavy metals from aluminum anodic oxidation wastewaters by membrane filtration. *Environ. Sci. Pollut. Res.* **25,** 22259–22272 (2018).

12. Qin, X. Y., Chai, M. R., Ju, D. Y. & Hamamoto, O. Investigation of plating wastewater treatment technology for chromium, nickel and copper. *IOP Conf. Ser. Earth Environ. Sci.* **191,** (2018).

13. Ismail, I., Soliman, A., Abdel-Monem, N., Ahmed, H. S. & Sorour, M. H. Nickel removal from electroplating waste water using stand-alone and electrically assisted ion exchange processes. *Int. J. Environ. Sci. Technol.* **11,** 199–206 (2014).

14. Ya, V., Martin, N., Chou, Y. H., Chen, Y. M., Choo, K. H., Chen, S. S. & Li, C. W. Electrochemical treatment for simultaneous removal of heavy metals and organics from surface finishing wastewater using sacrificial iron anode. *J. Taiwan Inst. Chem. Eng.* **83,** 107–114 (2018).

15. Zhu, Y., Fan, W., Zhou, T. & Li, X. Removal of chelated heavy metals from aqueous solution: a review of current methods and mechanisms. *Sci. Total Environ.* **678,** 253–266 (2019).

16. Kookana, R. S., Sarmah, A. K., Van Zwieten, L., Krull, E. & Singh, B. *Biochar application to soil. agronomic and environmental benefits and unintended consequences*. *Adv. Agron.* **112,** (Elsevier Inc., 2011).

17. Franca, A. S., Oliveira, L. S. & Ferreira, M. E. Kinetics and equilibrium studies of methylene blue adsorption by spent coffee grounds. *Desalination* **249,** 267–272 (2009).

18. Chen, B. & Chen, Z. Sorption of naphthalene and 1-naphthol by biochars of orange peels with different pyrolytic temperatures. *Chemosphere* **76,** 127–133 (2009).

19. Alslaibi, T. M., Abustan, I., Ahmad, M. A. & Foul, A. A. A review: production of activated carbon from agricultural byproducts via conventional and microwave heating. *J. Chem. Technol. Biotechnol.* **88,** 1183–1190 (2013).

20. National Institute of Statistics - INE. Agricultural production. (2018). at <https://www.pordata.pt/Portugal>

21. El-Fadel, M., Findikakis, A. N. & Leckie, J. O. Environmental impacts of solid waste landfilling. *J. Environ. Manage.* **50,** 1–25 (1997).

22. República Federativa do Brasil. *Lei No 12.305, de 2 de agosto de 2010.* 1–18 (2010). at <http://www.planalto.gov.br/ccivil_03/_ato2007-2010/2010/lei/l12305.htm>

23. MAOTDR - Ministério do Ambiente Ordenamento do Território e do Desenvolvimento Regional. *Plano Estratégico para os Resíduos Sólidos Urbanos (PERSU 2020)*. *Diário da República* 1–86 (2014).

24. AlOthman, Z. A., Habila, M. A., Ali, R., Abdel Ghafar, A. & El-din Hassouna, M. S. Valorization of two waste streams into activated carbon and studying its adsorption kinetics, equilibrium isotherms and thermodynamics for methylene blue removal. *Arab. J. Chem.* **7,** 1148–1158 (2014).

25. Izquierdo, L. & Sendra, J. M. in *Encycl. Food Sci. Nutr.* 1335–1341 (2004).

doi:10.1016/b0-12-227055-x/00241-8

26. Dugo, G. & Di Giacomo, A. *Citrus: the genus citrus*. (Taylor & Francis, 2002).

27. FAO. *Citrus fruit fresh and processed statistical bulletin 2016*. *Food Agric. Organ. United Nations* (2017). at <http://www.fao.org/3/a-i8092e.pdf>

28. National Institute of Statistics - INE. Agricultural Statistics 2017. 170 (2018). at <https://www.ine.pt/xportal/xmain?xpid=INE&xpgid=ine_publicacoes&PUBLICACOESpub_boui=320461359&PUBLICACOESmodo=2>

29. National Institute of Statistics - INE. Base de dados. (2018). at <www.ine.pt>

30. Ballistreri, G., Fabroni, S., Romeo, F. V., Timpanaro, N., Amenta, M. & Rapisarda, P. in *Polyphenols in plants* (ed. Watson, R.) 191–215 (Elsevier Inc., 2019). doi:10.1016/C2017-0-00209-4

31. Satari, B. & Karimi, K. Citrus processing wastes: environmental impacts, recent advances, and future perspectives in total valorization. *Resour. Conserv. Recycl.* **129,** 153–167 (2018).

32. Sharma, K., Mahato, N., Cho, M. H. & Lee, Y. R. Converting citrus wastes into value-added products: economic and environmently friendly approaches. *Nutrition* **34,** 29–46 (2017).

33. Adinaveen, T., Kennedy, L. J., Vijaya, J. J. & Sekaran, G. Studies on structural, morphological, electrical and electrochemical properties of activated carbon prepared from sugarcane bagasse. *J. Ind. Eng. Chem.* **19,** 1470–1476 (2013).

34. Bridgwater, A. V. Review of fast pyrolysis of biomass and product upgrading. *Biomass and Bioenergy* **38,** 68–94 (2012).

35. Angin, D., Altintig, E. & Köse, T. E. Influence of process parameters on the surface and chemical properties of activated carbon obtained from biochar by chemical activation. *Bioresour. Technol.* **148,** 542–549 (2013).

36. Afroze, S. & Sen, T. K. A review on heavy metal ions and dye adsorption from water by agricultural solid waste adsorbents. *Water. Air. Soil Pollut.* **229,** (2018).

37. Kadirvelu, K. & Namasivayam, C. Activated carbon from coconut coirpith as metal adsorbent: adsorption of Cd(II) from aqueous solution. *Adv. Environ. Res.* **7,** 471–478 (2003).

38. Gautam, R. K., Mudhoo, A., Lofrano, G. & Chattopadhyaya, M. C. Biomass-derived biosorbents for metal ions sequestration: adsorbent modification and activation methods and adsorbent regeneration. *J. Environ. Chem. Eng.* **2,** 239–259 (2014).

39. Özsin, G., Kılıç, M., Apaydın-Varol, E. & Pütün, A. E. Chemically activated carbon

production from agricultural waste of chickpea and its application for heavy metal adsorption: equilibrium, kinetic, and thermodynamic studies. *Appl. Water Sci.* **9,** 1–14 (2019).

40. Jain, A., Balasubramanian, R. & Srinivasan, M. P. Hydrothermal conversion of biomass waste to activated carbon with high porosity: a review. *Chem. Eng. J.* **283,** 789–805 (2016).

41. Román, S., Libra, J., Berge, N., Sabio, E., Ro, K., Li, L., Ledesma, B., Alvarez, A. & Bae, S. Hydrothermal carbonization: modeling, final properties design and applications: a review. *Energies* **11,** 1–28 (2018).

42. Berge, N. D., Ro, K. S., Mao, J., Flora, J. R. V., Chappell, M. A. & Bae, S. Hydrothermal carbonization of municipal waste streams. *Environ. Sci. Technol.* **45,** 5696–5703 (2011).

43. Román, S., Valente Nabais, J. M., Ledesma, B., González, J. F., Laginhas, C. & Titirici, M. M. Production of low-cost adsorbents with tunable surface chemistry by conjunction of hydrothermal carbonization and activation processes. *Microporous Mesoporous Mater.* **165,** 127–133 (2013).

44. Zhang, B., Heidari, M., Regmi, B., Salaudeen, S., Arku, P., Thimmannagari, M. & Dutta, A. Hydrothermal carbonization of fruit wastes: a promising technique for generating hydrochar. *Energies* **11,** 1–14 (2018).

45. Schimmelpfennig, S. & Glaser, B. One step forward toward characterization: some important material properties to distinguish biochars. *J. Environ. Qual.* **41,** 1001–1013 (2012).

46. Mäkelä, M., Benavente, V. & Fullana, A. Hydrothermal carbonization of industrial mixed sludge from a pulp and paper mill. *Bioresour. Technol.* **200,** 444–450 (2016).

47. Jin, F., Wang, Y., Zeng, X. & Shen, Z. in *Appl. Hydrothermal React. to Biomass Convers.* (ed. Jin, F.) 3–28 (Springer Berlin Heidelberg, 2014). doi:10.1007/978-3-642-54458-3

48. Marsh, H. & Reinoso, F. R. *Activated carbon*. (Elsevier, 2006). doi:10.1016/B978-0-08-044463-5.X5013-4

49. Hu, B., Yu, S.-H., Wang, K., Liu, L. & Xu, X.-W. Functional carbonaceous materials from hydrothermal carbonization of biomass: an effective chemical process. *Dalt. Trans.* **9226,** 5414–5423 (2008).

50. Hu, B., Wang, K., Wu, L., Yu, S. H., Antonietti, M. & Titirici, M. M. Engineering carbon materials from the hydrothermal carbonization process of biomass. *Adv. Mater.* **22,** 813–828 (2010).

51. Erdogan, E., Atila, B., Mumme, J., Reza, M. T., Toptas, A., Elibol, M. & Yanik, J.

Characterization of products from hydrothermal carbonization of orange pomace including anaerobic digestibility of process liquor. *Bioresour. Technol.* **196,** 35–42 (2015).

52. Reza, M. T., Uddin, M. H., Lynam, J. G., Hoekman, S. K. & Coronella, C. J. Hydrothermal carbonization of loblolly pine: reaction chemistry and water balance. *Biomass Convers. Biorefinery* **4,** 311–321 (2014).

53. Von Loesecke, H. W. Citrus fruit industry. *Ind. Eng. Chem.* **44,** 476–482 (1952).

54. Chavan, P., Singh, A. K. & Kaur, G. Recent progress in the utilization of industrial waste and by-products of citrus fruits: a review. *J. Food Process Eng.* **41,** 1–10 (2018).

55. Tran, H. N., You, S. J. & Chao, H. P. Effect of pyrolysis temperatures and times on the adsorption of cadmium onto orange peel derived biochar. *Waste Manag. Res.* **34,** 129–138 (2016).

56. Sudha, R., Srinivasan, K. & Premkumar, P. Kinetic, mechanism and equilibrium studies on removal of Pb(II) using Citrus limettioides peel and seed carbon. *Res. Chem. Intermed.* **42,** 1677–1697 (2016).

57. Mohammadi, S. Z., Karimi, M. A., Yazdy, S. N., Shamspur, T. & Hamidian, H. Removal of Pb(II) ions and malachite green dye from wastewater by activated carbon produced from lemon peel. *Quim. Nova* **37,** 804–809 (2014).

58. Naik, R. M., Ratan, S. & Singh, I. Use of orange peel as an adsorbent for the removal of Cr(VI) from its aqueous solution. *Indian J. Chem. Technol.* **25,** 300–305 (2018).

59. Bhatnagar, A., Minocha, A. K. & Sillanpää, M. Adsorptive removal of cobalt from aqueous solution by utilizing lemon peel as biosorbent. *Biochem. Eng. J.* **48,** 181–186 (2010).

60. Moreno-Piraján, J. C. & Giraldo, L. Heavy metal ions adsorption from wastewater using activated carbon from orange peel. *E-Journal Chem.* **9,** 926–937 (2012).

61. Han, C. H., Zhang, R. M., Cheng, T. & Zhang, X. Effect of activated carbon prepared from grapefruit peel on the treatment of heavy metal copper. *DEStech Trans. Eng. Technol. Res.* 2270–2276 (2017). doi:10.12783/dtetr/apetc2017/11456

62. Fernandez, M. E., Ledesma, B., Román, S., Bonelli, P. R. & Cukierman, A. L. Development and characterization of activated hydrochars from orange peels as potential adsorbents for emerging organic contaminants. *Bioresour. Technol.* **183,** 221–228 (2015).

63. Ali, M. H. H. & Abdel-Satar, A. M. Removal of some heavy metals from aqueous solutions using natural wastes orange peel activated carbon. *IJRDO-Journal Appl. Sci.* **3,** 13–30 (2017).

64. Berk, Z. in *Citrus Fruit Process.* 1–8 (2016). doi:10.1016/b978-0-12-803133-9.00001-1

65. Pascual, J. M. & Carmona, J. F. Composition of citrus pulp. *Anim. Feed Sci. Technol.* **5,** 1–10 (1980).

66. Zema, D. A., Calabrò, P. S., Folino, A., Tamburino, V., Zappia, G. & Zimbone, S. M. Valorization of citrus processing waste : a review. *Waste Manag.* **80,** 252–273 (2018).

67. Guiza, S. Biosorption of heavy metal from aqueous solution using cellulosic waste orange peel. *Ecol. Eng.* **99,** 134–140 (2017).

68. Torab-Mostaedi, M., Asadollahzadeh, M., Hemmati, A. & Khosravi, A. Equilibrium, kinetic, and thermodynamic studies for biosorption of cadmium and nickel on grapefruit peel. *J. Taiwan Inst. Chem. Eng.* **44,** 295–302 (2013).

69. Nasernejad, B., Zadeh, T. E., Pour, B. B., Bygi, M. E. & Zamani, A. Camparison for biosorption modeling of heavy metals (Cr (III), Cu (II), Zn (II)) adsorption from wastewater by carrot residues. *Process Biochem.* **40,** 1319–1322 (2005).

70. Pathak, P. D., Mandavgane, S. A. & Kulkarni, B. D. Fruit peel waste: characterization and its potential uses. *Curr. Sci.* **113,** 444–454 (2017).

71. Koller, M. & Saleh, H. M. in *Heavy Met.* 13 (InTech, 2018). doi:10.5772/intechopen.74783

72. Mertz, W. The essential trace elements. *Science (80-.).* **213,** 1332–1338 (1981).

73. Kumar, S. & Trivedi, A. V. A review on role of nickel in the biological system. *Int. J. Curr. Microbiol. Appl. Sci.* **5,** 719–727 (2016).

74. Zhao, J., Shi, X., Castranova, V. & Ding, M. Occupational toxicology of nickel and nickel compounds. *J. Environ. Pathol. Toxicol. Oncol.* **28,** 177–208 (2009).

75. Bencko, V. Nickel: a review of its occupational and environmental toxicology. *J. Hyg. Epidemiol. Microbiol. Immunol.* **27,** 237–47 (1983).

76. Kinhikar, V. R. Removal of Nickel (II) from aqueous solutions by adsorption with granular activated carbon (GAC). *Res. J. Chem. Sci.* **2,** 6–11 (2012).

77. Bartczak, P., Norman, M., Klapiszewski, Ł., Karwańska, N., Kawalec, M., Baczyńska, M., Wysokowski, M., Zdarta, J., Ciesielczyk, F. & Jesionowski, T. Removal of nickel(II) and lead(II) ions from aqueous solution using peat as a low-cost adsorbent: a kinetic and equilibrium study. *Arab. J. Chem.* **11,** 1209–1222 (2018).

78. Mansour, S. E. & Hasieb, I. H. Removal of nickel from drinking water by

electrocoagulation technique using alternating current. *Curr. Res. Chem.* **4,** 41–50 (2012).

79. National Council for the Environment - CONAMA. *Resolution nº 357*. 23 (2005).

80. Ministry of the Environment. *Decree-law nº 236*. 47 (1998).

81. World Health Organization - WHO. Nickel in drinking-water. *Environ. Heal.* 1–30 (2005). doi:10.1016/j.kjms.2011.05.002

82. Ruthven, D. M. *Principles of adsorption and adsorption process*. (John Willey & Sons, Inc., 1984).

83. Nascimento, R. F., Lima, A. C. A., Vidal, C. B., Melo, D. Q. & Cabral Raulino, G. S. *Adsorção: aspectos teóricos e aplicações ambientais*. *Imprensa Univ. da Univ. Fed. do Ceará* (Editora UFC, 2014). doi:10.13140/RG.2.1.4340.1041

84. Wang, S., Wang, K., Dai, C., Shi, H. & Li, J. Adsorption of Pb2+ on amino-functionalized core-shell magnetic mesoporous SBA-15 silica composite. *Chem. Eng. J.* **262,** 897–903 (2015).

85. Tan, X., Liu, Y., Zeng, G., Wang, X., Hu, X., Gu, Y. & Yang, Z. Application of biochar for the removal of pollutants from aqueous solutions. *Chemosphere* **125,** 70–85 (2015).

86. Mahdi, Z., Yu, Q. J. & El Hanandeh, A. Competitive adsorption of heavy metal ions (Pb 2+, Cu 2+, and Ni 2+) onto date seed biochar: batch and fixed bed experiments. *Sep. Sci. Technol.* **54,** 888–901 (2019).

87. Shukla, S. R. & Pai, R. S. Adsorption of Cu(II), Ni(II) and Zn(II) on modified jute fibres. *Bioresour. Technol.* **96,** 1430–1438 (2005).

88. Samarghandi, M. R., Siboni, M. S., Jafari, S. J. & Rahimi, S. Removal of divalent nickel from aueous solution by adsorption onto modified holly sawdust. *Iran. J. Environ. Heal. Sci.Eng., 2011* **8,** 181–188 (2011).

89. Erdoğan, S., Önal, Y., Akmil-Başar, C., Bilmez-Erdemoğlu, S., Sarici-Özdemir, Ç., Köseoğlu, E. & IçDuygu, G. Optimization of nickel adsorption from aqueous solution by using activated carbon prepared from waste apricot by chemical activation. *Appl. Surf. Sci.* **252,** 1324–1331 (2005).

90. Mo, J., Yang, Q., Zhang, N., Zhang, W., Zheng, Y. & Zhang, Z. A review on agro-industrial waste (AIW) derived adsorbents for water and wastewater treatment. *J. Environ. Manage.* **227,** 395–405 (2018).

91. Soares, M. R. & Casagrande, J. C. in *Tópicos em Ciência do Solo* (eds. Ribeiro, M. R., Nascimento, C. W. A. do, Ribeiro Filho, M. R. & Cantalice, J. R. B.) 85–95 (2009).

92. Ho, Y. S. & McKay, G. A Comparison of chemisorption kinetic models applied to pollutant removal on various sorbents. *Process Saf. Environ. Prot.* **76,** 332–340 (1998).

93. Miao, M. S., Liu, Q., Shu, L., Wang, Z., Liu, Y. Z. & Kong, Q. Removal of cephalexin from effluent by activated carbon prepared from alligator weed: kinetics, isotherms, and thermodynamic analyses. *Process Saf. Environ. Prot.* **104,** 481–489 (2016).

94. Ho, Y.-S. Review of second-order models for adsorption systems. *J. Hazard. Mater.* **136,** 681–9 (2006).

95. Chen, Y., Wang, H., Zhao, W. & Huang, S. Four different kinds of peels as adsorbents for the removal of Cd (II) from aqueous solution: kinetics, isotherm and mechanism. *J. Taiwan Inst. Chem. Eng.* **88,** 146–151 (2018).

96. Sadeek, S. A., Negm, N. A., Hefni, H. H. H. & Abdel Wahab, M. M. Metal adsorption by agricultural biosorbents: adsorption isotherm, kinetic and biosorbents chemical structures. *Int. J. Biol. Macromol.* **81,** 400–409 (2015).

97. Elhafez, S. E. A., Hamad, H. A., Zaatout, A. A. & Malash, G. F. Management of agricultural waste for removal of heavy metals from aqueous solution: adsorption behaviors, adsorption mechanisms, environmental protection, and techno-economic analysis. *Environ. Sci. Pollut. Res.* **24,** 1397–1415 (2017).

98. Melia, P. M., Busquets, R., Ray, S. & Cundy, A. B. Agricultural wastes from wheat, barley, flax and grape for the efficient removal of Cd from contaminated water. *RSC Adv.* **8,** 40378–40386 (2018).

99. Chien, S. H. & Clayton, W. R. Application of Elovich Equation to the Kinetics of Phosphate Release and Sorption in Soils. *Soil Sci. Soc. Am. J.* **44,** 265–268 (1980).

100. Liu, Z. rong, Zhou, L. min, Wei, P., Zeng, K., Wen, C. xi & Lan, H. hua. Competitive adsorption of heavy metal ions on peat. *J. China Univ. Min. Technol.* **18,** 255–260 (2008).

101. Ho, Y. S. & McKay, G. Application of kinetic models to the sorption of copper (II) on to peat. *Adsorpt. Sci. Technol.* **20,** 797–815 (2002).

102. Largitte, L. & Pasquier, R. A review of the kinetics adsorption models and their application to the adsorption of lead by an activated carbon. *Chem. Eng. Res. Des.* **109,** 495–504 (2016).

103. Manonmani, M., Manjuladevi, R. & Anitha, S. Kinetic study on adsorption of Cr (VI), Ni (II), Cd (II) and Pb (II) ions from aqueous solutions using activated carbon prepared from Cucumis melo peel. *Appl. Water Sci.* **36,** 1–8 (2018).

104. Giles, C. H., Smith, D. & Huitson, A. A general treatment and classification of the solute adsorption isotherm. **47,** (1974).

105. Hinz, C. Description of sorption data with isotherm equations. *Geoderma* 225–243 (2001).

106. Langmuir, I. The adsorption of gases on plane surfaces of glass, mica and platinum. *J. Am. Chem. Soc.* **40,** 1361–1403 (1918).

107. Soares, M. R. & Casagrande, J. C. in *Tópicos em Ciência do Solo* (eds. Ribeiro, M. R., Nascimento, C. W. A. do, Ribeiro Filho, M. R. & Cantalice, J. R. B.) 105–150 (2009).

108. Sposito, G. Use of the Langmuir equation in the interpretation of “adsorption” phenomena. *Soil Sci. Soc. Am. J.* **46,** 1147 (2010).

109. Bibaj, E., Lysigaki, K., Nolan, J. W., Seyedsalehi, M., Deliyanni, E. A., Mitropoulos, A. C. & Kyzas, G. Z. Activated carbons from banana peels for the removal of nickel ions. *Int. J. Environ. Sci. Technol.* **16,** 667–680 (2019).

110. Freundlich, H. Adsorption in lösungen. *Zeitschrift Für Phys. Chemie* **57,** 385–470 (1907).

111. Sposito, G. Derivation of the Freundlich equation for ion exchange reactions in soils. *Soil Sci. Soc. Am. J.* **44,** 652 (1980).

112. Awoyemi, A. Understanding the adsorption of polycyclic aromatic hydrocarbons from aqueous phase onto activated carbon. *Master’s Thesis, Dep. Chem. Eng. Appl. Chem. Univ. Toronto* (2011). at <https://tspace.library.utoronto.ca/bitstream/1807/30169/6/Awoyemi_Ayodeji_O_201111_MASc_thesis.pdf>

113. Singh, S. & Shukla, S. R. Theoretical studies on adsorption of Ni(II) from aqueous solution using Citrus limetta peels. *Environ. Prog. Sustain. Energy* **36,** 864–872 (2017).

114. Tóth, J. A uniform interpretation of gas/solid adsorption. *J. Colloid Interface Sci.* **79,** 85–95 (1981).

115. Benzaoui, T., Selatnia, A. & Djabali, D. Adsorption of copper (II) ions from aqueous solution using bottom ash of expired drugs incineration. *Adsorpt. Sci. Technol.* **36,** 114–129 (2018).

116. Rangabhashiyam, S., Anu, N., Giri Nandagopal, M. S. & Selvaraju, N. Relevance of isotherm models in biosorption of pollutants by agricultural byproducts. *J. Environ. Chem. Eng.* **2,** 398–414 (2014).

117. Vijayaraghavan, K., Padmesh, T. V. N., Palanivelu, K. & Velan, M. Biosorption of nickel(II) ions onto Sargassum wightii: Application of two-parameter and three-parameter isotherm models. *J. Hazard. Mater.* **133,** 304–308 (2006).

118. Brdar, M., Šćiban, M., Takači, A. & Došenović, T. Comparison of two and three parameters adsorption isotherm for Cr(VI) onto Kraft lignin. *Chem. Eng. J.* **183,** 108–111 (2012).

119. Thi, T. T. L. & Van, K. Le. Adsorption behavior of Pb (II) in aqueous solution using coffee husk-based activated carbon modified by nitric acid American Journal of Engineering Research (AJER). *Am. J. Eng. Res.* **5,** 120–129 (2016).

120. Chang, C. F., Chang, C. Y. & Tsai, W. T. Effects of burn-off and activation temperature on preparation of activated carbon from corn cob agrowaste by CO2 and steam. *J. Colloid Interface Sci.* **232,** 45–49 (2000).

121. Chen, Y., Huang, B., Huang, M. & Cai, B. On the preparation and characterization of activated carbon from mangosteen shell. *J. Taiwan Inst. Chem. Eng.* **42,** 837–842 (2011).

122. Teng, H. & Lin, H. C. Activated carbon production from low ash subbituminous coal with CO2 activation. *AIChE J.* **44,** 1170–1177 (1998).

123. Fałtynowicz, H., Kaczmarczyk, J. & Kułazyński, M. Preparation and characterization of activated carbons from biomass material - Giant knotweed (Reynoutria sachalinensis). *Open Chem.* **13,** 1150–1156 (2015).

124. Rodriguez-Reinoso, F., Lopez-Gonzalez, J. D. & Berenguer, C. Activates carbons from almond shells: preparation and characterization by nitrogen adsorption. *Carbon N. Y.* **20,** 513–518 (1981).

125. Hamzaoui, M., Bestani, B. & Benderdouche, N. The use of linear and nonlinear methods for adsorption isotherm optimization of basic green 4-dye onto sawdust-based activated carbon. *J. Mater. Environ. Sci.* **9,** 1110–1118 (2018).

126. Hadi, M., McKay, G., Samarghandi, M. R., Maleki, A. & Aminabad, M. S. Prediction of optimum adsorption isotherm: Comparison of chi-square and Log-likelihood statistics. *Desalin. Water Treat.* **49,** 81–94 (2012).

127. Kissell, R. & Poserina, J. in *Optim. Sport. Math, Stat. Fantasy* 39–67 (Academic Press, 2017). doi:10.1016/b978-0-12-805163-4.00002-5

128. Wojciechowski, B. W. & Rice, N. M. in *Exp. methods kinectic Stud.* 211–222 (Elsevier B.V, 2003).

129. Lim, W. C., Srinivasakannan, C. & Balasubramanian, N. Activation of palm shells by phosphoric acid impregnation for high yielding activated carbon. *J. Anal. Appl. Pyrolysis* **88,** 181–186 (2010).

130. Moreno-Piraján, J. C. & Giraldo, L. Activated carbon from bamboo waste modified with iron and its application in the study of the adsorption of arsenite and arsenate. *Cent. Eur. J. Chem.* **11,** 160–170 (2013).

131. Liu, D., Jia, B., Liu, X., Zhao, B., Gao, J., Cao, Q., Wu, S. & Qin, Y. Effects of oxygen functional groups and FeCl3 on the evolution of physico-chemical structure in activated carbon obtained from Jixi bituminous coal. *RSC Adv.* **8,** 8569–8579 (2018).

132. Hamid, S. B. A., Teh, S. J. & Lim, Y. S. Catalytic hydrothermal upgrading of α-cellulose using iron salts as a lewis acid. *BioResources* **10,** 5974–5986 (2015).

133. Gong, X., Guo, Z. & Wang, Z. Variation of char structure during anthracite pyrolysis catalyzed by Fe2O3 and its influence on char combustion reactivity. *Energy and Fuels* **23,** 4547–4552 (2009).

134. Couto, G. M., Dessimoni, A. L. de A., Bianchi, M. L., Perígolo, D. M. & Trugilho, P. F. Use of sawdust Eucalyptus sp. in the preparation of activated carbons. *Ciência e Agrotecnlogia* **36,** 69–77 (2012).

135. Chattopadhyaya, G., Macdonald, D. G., Bakhshi, N. N., Mohammadzadeh, J. S. S. & Dalai, A. K. Preparation and characterization of chars and activated carbons from Saskatchewan lignite. *Fuel Process. Technol.* **87,** 997–1006 (2006).

136. Wen, C. Y. & Dutta, S. in *Coal Convers. Technol.* (eds. Wen, C. Y. & Lee, E. S.) 57–170 (Addison-Wesley Publishing Co., 1979).

137. Bautista-Toledo, I., Ferro-García, M. A., Rivera-Utrilla, J., Moreno-Castilla, C. & Fernández, F. J. V. Bisphenol A removal from water by activated carbon. Effects of carbon characteristics and solution chemistry. *Environ. Sci. Technol.* **39,** 6246–6250 (2005).

138. Bansal, R. C. & Goyal, M. *Activated Carbon Adsorption*. (Taylor & Francis, 2005).

139. Boehm, H. P. Some aspects of the surface chemistry of carbon blacks and other carbons. *Carbon N. Y.* **32,** 759–769 (1994).

140. Godino-Salido, M. L., López-Garzón, R., Gutiérrez-Valero, M. D., Arranz-Mascarós, P., Melguizo-Guijarro, M., López De La Torre, M. D., Gómez-Serrano, V., Alexandre-Franco, M., Lozano-Castelló, D., Cazorla-Amorós, D. & Domingo-García, M. Effect of the surface chemical groups of activated carbons on their surface adsorptivity to aromatic adsorbates based on π-π Interactions. *Mater. Chem. Phys.* **143,** 1489–1499 (2014).

141. Largitte, L., Brudey, T., Tant, T., Dumesnil, P. C. & Lodewyckx, P. Microporous and Mesoporous Materials Comparison of the adsorption of lead by activated carbons from three lignocellulosic precursors. *Microporous Mesoporous Mater.* **219,** 265–275 (2016).

142. Mattson, J. A., Mark, H. B., Malbin, M. D., Weber, W. J. & Crittenden, J. C. Surface chemistry of active carbon: Specific adsorption of phenols. *J. Colloid Interface Sci.* **31,** 116–130 (1969).

143. Menéndez, J. A., Phillips, J., Xia, B. & Radovic, L. R. On the modification and characterization of chemical surface properties of activated carbon: In the search of carbons with stable basic properties. *Langmuir* **12,** 4404–4410 (1996).

144. Kumar, P. S., Ramalingam, S., Dinesh Kirupha, S., Murugesan, A., Vidhyadevi, T. & Sivanesan, S. Adsorption behavior of nickel(II) onto cashew nut shell : Equilibrium , thermodynamics , kinetics , mechanism and process design. *Chem. Eng. J.* **167,** 122–131 (2011).

145. Rodríguez-Estupiñán, P., Giraldo, L. & Moreno-Piraján, J. Nickel(II) ion adsorption onto activated carbon. Relationship between physicochemical properties and adsorption capacity. *Adsorpt. Sci. Technol.* **29,** 541–551 (2011).

146. Oliveira, L. C. A., Pereira, E., Guimaraes, I. R., Vallone, A., Pereira, M., Mesquita, J. P. & Sapag, K. Preparation of activated carbons from coffee husks utilizing FeCl3 and ZnCl2 as activating agents. *J. Hazard. Mater.* **165,** 87–94 (2009).

147. Periasamy, K. & Namasivayam, C. Removal of nickel(II) from aqueous solution and nickel plating industry wastewater using an agricultural waste: Peanut hulls. *Waste Manag.* **15,** 63–68 (1995).

148. Taty-Costodes, V. C., Fauduet, H., Porte, C. & Delacroix, A. Removal of Cd(II) and Pb(II) ions, from aqueous solutions, by adsorption onto sawdust of Pinus sylvestris. *J. Hazard. Mater.* **105,** 121–142 (2003).

COMMUNICATIONS

Marques, V. C., Diaz de Tuesta, J. L., Gomes, H. T., Dal Bosco, T. C.; Valorização da casca de citrinos na preparação de adsorventes para o tratamento de água. In: **2ª Escola de verão e Simpósio de Dupla Diplomação**, Instituto Politécnico de Bragança, July 1st to 3rd 2019. Oral presentation.

Marques, V. C., Diaz de Tuesta, J. L., Gomes, H. T., Dal Bosco, T. C.;. Carvões ativados a partir de cascas de citrinos para tratamento de águas residuais. In: **Encontro de Jovens Investigadores**. Instituto Politécnico de Bragança, December 5th 2019. Oral presentation.

Marques, V. C.; Shinibekova A.; Kalmakhanova M. S.; Diaz de Tuesta, J. L., Dal Bosco, T. C.; Massalimova, B. K.; Gomes, H. T.; Adsorption of Ni(II) on activated carbons prepared from tangerine peel by sequential hydrothermal carbonization and pyrolysis. In: **7th Portuguese Young Chemists Meeting**. Instituto Politécnico de Bragança. Delayed until 2021 for COVID-19 situation. Work submitted and accepted. May 20th to 22nd 2020.